# Structure-Reactivity Relationship for Titania Supported Vanadium-Phosphorous-Oxide Catalysts: ODH of Propane

*A thesis submitted in Partial Fulfillment of the*

*Requirements for the Degree of*

**Master of Technology**

*By*

***Rudra Pratap Singh***

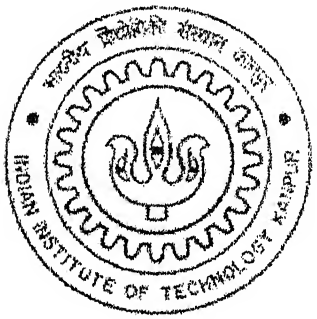


*to the*

**Department of Chemical Engineering**

**Indian Institute of Technology Kanpur, INDIA**

*April, 2004*

Dedicated

*To*

**My Beloved**

# Shyama Didi

# CERTIFICATE

It is certified that the work contained in the thesis entitled *Structure-Reactivity Relationship for Titania Supported Vanadium-Phosphorous-Oxide Catalysts: ODH of Propane by* Rudra Pratap Singh, has been carried out under my supervision and that this work has not been submitted elsewhere for a degree.

Dr. Goutam Deo
Associate Professor
Department of Chemical Engg.
Indian Institute of Technology Kanpur
Kanpur, INDIA
April, 2004

# Acknowledgements

I would like to express my deep sense of gratitude towards my Thesis Supervisor Dr. Goutam Deo for his valuable guidance, unflinching co-operation and everlasting patience through out my thesis work. I express my sincere gratefulness to him for the trust he had on me, for motivating me and for the moral support he extended to me always. I cherish the times that I spent with him as my supervisor.

I would like to extend my thanks to Dr. Deepak Kunzru for allowing me to perform some experimental works in their lab and Ms. Mahuya Dey for her unvaluable help during experiments. I would like to thank all the official and non-official people of Chemical Engineering department. I express my thanks towards Mr. Umashankar of XRD, Mr. Sharma and Mr. Pal of ACMS, Mr. Kanojia and Dr. Veena of EPR lab, Mr. B.K. Jha of Import Section for their help and a note of thanks to Mr. Hemant (Lab Assistant).

I thank my Lab mates, Laxman, Kamalakanta, Mallesh, Priyanka, Debaprasad and Girish for their help rendered to me through out my thesis work. Special note of thank to my friends Sukalyan and Manoj for their moral support and love to me always. Support extended by many other friends in my thesis work is noteworthy.

Finally I am indebted towards my family especially to my parents, without their blessings my thesis work would not have been completed successfully. I would like their love, help and faith in every aspect of my life.

**Rudra Pratap Singh**

# Contents

# List Of Tables

# List Of Figures

# ABSTRACT

*The effect of phosphorous as a modifier for 3%$V_2O_5/TiO_2$ was studied for the oxidative dehydrogenation (ODH) of propane. For this purpose several ratios of vanadium to phosphorous (2: 1, 1: 1 and 1: 2) catalysts were prepared by the incipient wetness impregnation method using co-precipitation onto a titania support from a solution containing vanadium and phosphorous ions. The catalysts samples were characterized by various techniques. The surface areas and X-Ray Diffraction patterns of the catalysts samples remained almost constant suggesting that the support is not significantly affected during preparation and no new crystalline phase is present. Electron Paramagnetic Resonance studies revealed the presence of paramagnetic vanadium oxide species in the unmodified and P-modified samples. The Temperature Programmed Reduction (TPR) results show the decrease in reducibility of unmodified samples and the formation of a new reducible phase for the sample containing vanadium to phosphorous ratio of 1:2. Reactivity studies were performed for the ODH of propane and it was observed that the conversion and selectivities of the catalysts depend upon the vanadium to phosphorous molar ratios. Contact time studies reveal that with the increase in vanadium to phosphorous ratio the conversion decreases and the propene selectivity at iso-conversion decreases. Furthermore, with an increase in propane conversion the propene selectivity decreases for all catalysts.*

*Two power law (PL) models and one mechanistic (MVK) model were considered to explain the reaction data. The kinetic-parameters are successfully estimated by minimization of an objective function using Genetic Algorithm. The PL-1 model considering propene as a primary product, and CO and $CO_2$ as secondary products described the reaction data better. From the kinetic-parameters obtained for the PL-1 and the corresponding MVK-1 model the effect of phosphorous modification was suggested. It was observed that progressive poisoning of the sites took place with phosphorous modification until a vanadium to phosphorous ratio of 1:2 for which a different mechanism with different activation energies occurred consistent with the TPR analysis. Using the kinetic-parameters the decrease in conversion with an increase in phosphorous modification was due to the progressive decrease in the rate constant of the primary ODH reaction. The increase in propene yield at iso-conversion with an increase in phosphorous modification was due to the decrease in the ratio of the rate constants for propene degradation to propene formation.*

# Chapter: 1

## *INTRODUCTION*

Owing to the low cost and environmental impact of light alkanes, functionalization of them has attracted considerable research interest. A potential area for alkane utilization is the conversion to unsaturated hydrocarbons since the current chemical industry depends heavily on the use of unsaturated hydrocarbons as starting material. Since the demand for these unsaturated hydrocarbons or light olefins is likely to significantly increase in the future and traditional sources of olefins production will no longer meet the demands. Thus, alternative ways to produce these important feedstocks have to be considered and developed.

Selective oxidation of light alkanes is one of the ways of transforming these relatively cheap natural products or byproducts into valuable chemicals. Among selective oxidation reactions the oxidative dehydrogenation (ODH) reaction is a special case and an attractive alternative to the classical dehydrogenation process. In the dehydrogenation process alkanes are directly converted over a catalyst to the olefins. In ODH, the thermodynamic characteristics of the double bond formation reaction are favorably modified with respect to the simple dehydrogenation reaction by the production of water molecule instead of hydrogen. The water molecule is a thermodynamically more favorable product and, consequently, the reaction is irreversible and goes 100 % completion.

Presently, dehydrogenation is used as the direct route for the production of lighter alkenes to high value olefins. In the case of propane dehydrogenation the reaction involved is

$C_3H_8 = C_3H_6 + H_2$ (1.1)

The enthalpy and Gibbs free energy of this reaction are

$\Delta H^0$ (700 K) = 128.8 kJ/mol and $\Delta G^0$ (700 K) = 32.1 kJ/mol

The enthalpy of the reaction suggests that this process is a highly endothermic process and requires severe conditions of high temperature (greater than $600^0$C). Furthermore, since there is an increase in the number of moles the reaction is favored at low pressure [1]. These severe conditions are also favorable for coke formation on the surface of the catalyst leading to catalyst deactivation. Consequently, deactivation dominates the reactor design since frequent decoking and regeneration of the catalyst has to be considered. In addition to practical considerations the reaction is also thermodynamically limited.

The ODH reaction using oxygen as oxidant is given by

$C_3H_8 + ½O_2 = C_3H_6 + H_2O$ (1.2)

The enthalpy and Gibbs free energy of this reaction are

$\Delta H^0$ (700 K) = -116.8 kJ/mol, $\Delta G^0$ (700 K) = -176.7 kJ/mol

The values of $\Delta H^0$ and $\Delta G^0$ make the reaction practically irreversible at all temperatures and eliminate the problem of coke formation. Furthermore, the ODH reaction being exothermic, it can be carried out at low temperature. Consequently, the ODH of propane would appear to be more efficient and less energy intensive for the formation of olefins. If ODH were the only reaction of importance then a catalyst could be found to maximize the rate of propane production. However, the ODH reaction performed in the presence of

oxygen also results in non-selective oxidation reactions, which are still more thermodynamically favorable compared to the desired alkenes. These total oxidation reactions strongly diminish the selectivities and yields, when the alkane conversion increases [1]. Another limitation of this reaction is its susceptibility to explosion due to the presence of oxygen. Thus, a catalyst is required that will give higher conversions at increased alkene selectivities.

The activation of the stable C–H bond of alkane at a low temperature while preserving the formed alkene from subsequent overoxidation is a prerequisite for a catalyst to be successful in the process. Among the catalysts that have been developed, vanadia containing catalysts are one of the more active and selective ones for the ODH of propane [2]. It has been widely used as an active component in mixed oxides and on supports for the ODH of propane. Supported vanadium oxide has gained much importance over the other catalysts due to their high degree of mechanical strength, better thermal stability and larger surface area [3]. The catalytic activity of vanadium oxide depends on their surface structure, character of chemical bond and the coordinative unsaturation of the surface atom among other factors.

Various characterization techniques have been applied to study the supported vanadium oxide phases on different metal oxides, such as Raman [4-9], solid-state $^{51}V$ NMR [10], UV-vis DRS [6-7,11], and EPR [9] spectroscopy. Using these characterization techniques it has been determined that the supported vanadia catalysts possess a two-dimensional surface species below monolayer loadings and the structure of the two dimensional surface species changes with loading. These surface vanadia species are responsible for the selective oxidation of alkane. For example, isolated $VO_4$ tetrahedra are observed on

catalysts supported on $TiO_2$, at very low vanadium loading. Polymeric vanadates are predominantly formed at high loadings in which each of the vanadium atoms has one terminal V=O bond, one, two or three V-O-V bonds, and two, one or zero V-O-M bonds [14]. The appearance of $V_2O_5$ crystallites is only observed at vanadium oxide coverages above the theoretical monolayer [10].

It is accepted that the vanadia species interact with the support in various forms depending on the nature of the support [22]. The surface vanadium oxide species on the support can be quite different from that of bulk $V_2O_5$. The acid–base character of the metal oxide support can determine both the nature of vanadium species and the catalytic behavior of these catalysts and therefore the distribution of the surface species, the metal–oxygen bond strength, and the mean distance between the vanadium active centers. These factors appear to be key for the catalytic performance of the supported vanadium oxide species. Basic supports tend to form stable mixed oxidic phases, while on acidic supports vanadia tends to disperse on the surface. Supports like alumina, zirconia, and titania allow good dispersion of surface vanadium oxide species.

Lemonidou et al [15] studied the ODH of propane over vanadia supported on different supports. Investigation of these catalysts on the propane ODH reaction revealed that the vanadia catalysts supported on $TiO_2$ are very active and follows the order: $V_2O_5/TiO_2 >> V_2O_5/ZrO_2 > V_2O_5/Al_2O_3 > V_2O_5/MgO$. The trends in activity is similar to the reducibility order obtained by $H_2$-TPR experiments. Similar trends in activity have also been reported by Arena et al [16]. The catalysts supported on $Al_2O_3$ are, however, the most selective. In all cases, an inverse relation of the conversion versus propene selectivity was observed. This relationship constitutes the major problem of the ODH

reaction since alkene productivity far less than that required for industrial application is achieved.

To tune the inverse relationship between conversion and selectivity several modifiers and additives are considered. The key factors that are to be controlled are the reducibility and the acid-base properties. The effect of the modifiers or additives should be such that the lattice oxygen of intermediate strength is achieved. Weakly bonded oxygen leads to over-oxidation and strongly bonded oxygen renders the catalyst inactive. Initially, it was realized that impurities (e.g. K, P, Si, sulfates) present on the surface of commercial titania pigments may influence the structure and catalytic properties of VTi catalysts. According to Deo and Wachs ([20-21] and references therein) some of the additives (e.g. $WO_3$, $SiO_2$, and $Nb_2O_5$) are anchored to the surface of the titania with lateral, indirect interactions with the vanadia surface species, whereas others (e.g. K or P) interact directly with the vanadia phase.

Vanadium-phosphorous mixed oxide (VPO) catalysts are promising catalysts for selective alkane activation for which they continue to attract considerable attention. In these systems it can be considered that the role of phosphorous is as a modifier for the vanadium phase. There are different VPO phases with vanadium in the +5, +4 and +3 oxidation state for which the structures have been resolved. The V (5+) phases correspond to hydrates, such as $VOPO_4.H_2O$ and $VOPO_4.2H_2O$, and phosphates, such as $VOPO_4$ ($\alpha_I$, $\alpha_{II}$, $\beta$, $\gamma$ and $\delta$). The V (4+) phases correspond to hydrogenophosphates, such as $VOHPO_4.0.5H_2O$, $VOHPO_4.4H_2O$ and $VO(H_2PO4)_2$, and to pyrophosphate $(VO)_2P_2O_7$ and metaphosphates $VO(PO_3)_2$. The V (3+) phases correspond to $VPO_4$, $V(PO_3)_3$ [23].

Out of all these VPO phases, vanadium pyrophosphates $(VO)_2P_2O_7$ and vanadium orthophosphates $VOPO_4$ has been considered in most studies. The catalyst activity of bulk VPO catalysts is increased by dispersing the active VPO phase on a support. The enhanced activity is not only due to the increase in surface area but also the interaction of the active phase and support. For example, Ciambelli et al studied [29] bulk and $TiO_2$-supported $(VO)_2P_2O_7$ for the ODH of C2–C4 hydrocarbons and observed better selectivity but low activity in these reactions for the supported system. Ciambelli and coworkers [29] did a comparative study of catalytic behavior of bulk and $TiO_2$-supported vanadium orthophosphate $VOPO_4.2H_2O$ and $Fe(H_2O)_{0.23}(VO)_{0.77}PO_4.2.3H_2O$ in ethane ODH. The activity of Ti-supported vanadium orthophosphate was more than two orders of magnitude higher than that shown by corresponding bulk catalysts. These studies also revealed that $Fe^{3+}$ substitution in vanadium orthophosphate results in considerable modification of both redox and acid properties for bulk materials, which leads to an improvement of catalytic performance in the ODH of ethane. This effect is less significant for $TiO_2$-supported catalysts due to the dominance of the strong effect of vanadium-titanium interaction that markedly influences both the reducibility and acidity of vanadyl phosphate.

The effect of supporting vanadium pyrophosphate on different oxides such as alumina, silica or titania has been widely investigated and results revealed that $TiO_2$ promotes the best dispersion of active phase [26-27]. Lisi et al [30] also reported good catalytic performance of submonolayer and monolayer $TiO_2$- and $\gamma$ -$Al_2O_3$- supported $VOPO_4$ in the ODH of ethane with $TiO_2$ being the support giving the best results. Monolayer dispersion of $VOPO_4$ on a suitable support provides an enhanced vanadium

reducibility related to a great increase of activity in the ODH of ethane. Savary and coworkers [31] studied the propane ODH over the $VPO/TiO_2$ catalyst between 300 and 400°C and obtained satisfactory performances. They enhanced the bronsted acid sites by addition of water or pyridine in the feed which resulted in better propene selectivity at the expense of $CO_x$ selectivity.

In these studies it appears that phosphorous modified vanadia-titania (VTi) catalyst is a potential system for the alkane ODH reaction. However, the reaction mechanism and kinetic-parameters involved for these systems have not been analyzed. Analysis of the reaction mechanism by knowledge of the kinetic-parameters would be beneficial for designing a proper catalyst to increase the alkene yield and to operate the reactor under optimal conditions. An appropriate combination of kinetic parameters would maximize the desired alkene product and minimize the undesired carbon oxides. Obtaining the kinetic-parameters requires a proper design and modeling of the reactor. Based on the solution of a series of ordinary differential equations initial values problems obtained from the reactor modeling the kinetic-parameters can be obtained by minimizing the difference between the actual and predicted outlet concentrations. Several techniques have been used for minimization of which genetic algorithms (GA) show promising results.

## 1.1 Objective of study

Thus, the present study is aimed at understanding the effect of phosphorous modification on the catalytic activity of $V_2O_5/TiO_2$ catalysts for the ODH of propane by estimating the kinetic-parameters of a chosen reaction scheme. To achieve this primary objective 3% $V_2O_5/TiO_2$, is chosen as the base catalyst for which the effect of phosphorous

modification is chosen. The 3% $V_2O_5/TiO_2$ catalyst is chosen since only surface active vanadium species are present. The vanadium to phosphorous ratio is varied to understand the effect of the modifier. The catalysts are initially characterized and then propane ODH is carried out over these catalysts. Three reaction models are proposed to explain the observed reaction data. The kinetic-parameters associated with these reactions models are determined by minimization of an objective function with the help of a GA optimization technique. The effect of phosphorous modification is understood by correlating the changes in kinetic-parameter with changes in structure as the phosphorous content is varied. Such type of analysis provides the structure-reactivity relationships of titania supported VPO catalysts for the ODH of propane.

## 1.2 Thesis organization

The thesis contains five chapters of which the current chapter is the first. The next chapter, Chapter 2, presents a brief literature review related to unmodified and phosphorous-modified VTi catalysts. The various methods used in the present study are reported in Chapter 3. The results obtained from the characterization studies, the analysis of the reaction of phosphorous modified and unmodified VTi catalysts for the ODH of propane and values of kinetic parameters obtained by GA are given in Chapter 4. The results obtained are also discussed in this chapter. Conclusions and recommendations for future work are reported in Chapter 5. In each chapter the Tables and Figures are given at the end. The references used throughout the thesis are given at the end and in numerical order as they appear in the text. The appendix is the last section and it provides the data obtained from the reaction studies.

# Chapter: 2

## *LITERATURE REVIEW*

In the last few years studies have been carried out on the structure and reactivity of ODH of propane over supported vanadia catalysts. Several studies have also been carried out over modified supported vanadia catalysts [17-21]. Interestingly, however, the effect of phosphorous modification on supported vanadia catalysts for the ODH of propane and the kinetic analysis of ODH reaction to explain the structure-reactivity relationship of phosphorous-modified vanadia catalysts has not been carried out. Kinetic analysis of the ODH reaction as a function of phosphorous modification requires the use of optimization techniques for kinetic-parameter estimation. Genetic algorithm is a recent tool used for the optimization of a objective function for kinetic-parameter estimation. A literature review on vanadia based catalyst, unsupported and supported phosphorous modified vanadium catalysts and kinetic-parameter estimation by genetic algorithm is given below with special reference to the ODH of alkanes.

## 2.1 Vanadium oxide based catalysis

Deo, Haber and Wachs [21] have proposed several fundamental ideas regarding the structure and reactivity of vanadium oxide species on the oxide supports. Ideas regarding vanadia species include information about the monolayer surface coverage, stability of monolayer, oxidation state, molecular structure, acidity and reactivity. They have also described physico-chemical characteristics of vanadia catalyst compared to other oxide catalysts.

Reddy [33] characterized the $V_2O_5$ supported on $TiO_2$ catalyst. Based on Raman spectroscopy, it is observed that monolayer coverage occurs at $4\%V_2O_5/TiO_2$. During the propane ODH reaction, the activity of propane increases up to monolayer coverage and then decreases for above monolayer coverages.

## 2.2 Unsupported VPO Catalysts

Vanadium phosphorous mixed oxides catalysts continue to attract considerable attention due to its capability to activate alkanes. However, the full potential of vanadium-phosphorous-oxide (V-P-O) catalysts has been barely investigated. In addition to the ODH reactions, VPO catalysts have also been reported as selective in the oxidation of butane to maleic anhydride, oxidation of propane and pentane to the corresponding acid and anhydride.

Al-Zahrani et al. [24] have investigated the catalytic effect of various metal pyrophosphates (i.e., $Mn_2P_2O_7$, $Ni_2P_2O_7$, $CeP_2O_7$, $Mg_2P_2O_7$, $ZrP_2O_7$, $Ba_2P_2O_7$, $V_4(P_2O_7)_3$ and $Cr_4(P_2O_7)_3$ on the oxidative dehydrogenation of isobutane to isobutene in the reaction temperature range of 400–600 $^0$C. $CeP_2O_7$ gave the highest isobutene yield and selectivity (71 %), however, $V_4(P_2O_7)_3$ was the most active catalyst with an isobutane conversion of 33.5 % at 500 $^0$C. Increasing the reaction temperature resulted in higher isobutane conversions and lower isobutene selectivity, whereas the reaction time was not so important, especially when isobutene conversion was limited to 11 % at 550 $^0$C. Working at temperatures higher than 550 $^0$C, the homogeneous gas phase reactions became significant and the oxygen conversion was about 100 %. The XRD results revealed that the pyrophosphate catalysts did not suffer from any structural modification

whereas FT-IR spectra indicated that the involvement of $P_2O_7$ group and adsorption of hydrocarbon species in the same ODH reaction was different for the different catalysts.

Jibril et. al. [25] studied the effect of the same metal pyrophosphate catalysts in the oxidative dehydrogenation of propane to propene. All catalysts showed increase in degrees of conversion and decrease in olefins selectivity with increase in reaction temperature. At 550 $^0$C, $MnP_2O_7$ exhibited the highest activity (40.7 % conversion) and total olefins ($C_3H_6$ and $C_2H_4$) yield (29.3 %). The other catalysts, indicated by their respective metals, may be ranked (based on olefins yield) as V (16.9 %) < Cr (17.5 %) < Ce (25.1 %) < Zr (26.2 %) < Ni (26.8 %) < Mg (27.9 %). The results suggested that the lattice oxygen plays a key role in the selectivity-determining step.

Loukh et al. [28] studied the oxidative dehydrogenation of ethane on V- and Cr-based phosphate catalysts at 550$^O$C. Vanadium and chromium cations were introduced in zirconium hydrogen phosphates either by cationic exchange of their acidic proton or by impregnation with $VO^{2+}$ and $Cr^{3+}$ and then compared to $(VO)_2P_2O_7$ and $CrPO_4$ pure phases. They observed that the catalytic activity for ethane ODH was proportional to the number of accessible cations and selectivity was dependent on the nature of the support and cation. They reported that $VO^{2+}$ and $Cr^{3+}$ on the $\alpha Zr(HPO_4)_2.2H_2O$ phase were more selective toward ethylene. The $(VO)_2P_2O_7$ and to a lesser extent $CrPO_4$ were even more selective toward ethylene at similar conversion levels. UV-VIS, ESR, XRD, IR, and SEM were used for the characterization of the catalysts. Based on the characterization study data, they concluded that the catalytic features were related to V and Cr local arrangements (small clusters or chain arrangements) and to the counter anion, $O^{2-}$ or

$PO_4^{3-}$. The best catalyst for ethane oxidative dehydrogenation consisted of $VO^{2+}$ and $Cr^{3+}$ chains separated by $PO_4^{3-}$ anions, which are stronger bases than $O^{2-}$ anions.

## 2.3 Supported VPO catalysts

The catalytic activity of bulk catalysts is dramatically increased by dispersing the active phase on a support due not only to the enhanced surface area but also to the interaction between active phase and support. Nakamura et al. [34] described the first supported V-P-O catalysts. They prepared alumina-supported catalysts for the selective oxidation of 1-butane to MA (maleic anhydride) and obtained reasonably high selectivities. The selectivity appeared to be enhanced by the average oxidation state of the active vanadium centers. Varma and Saraf [35] studied the selective oxidation of 1-butene over silica-gel supported V-P-O systems and found that MA could be obtained with reasonable selectivities.

Overbeek et al. [26] studied the butane oxidation reaction over a series of titania supported vanadia catalysts including the different loadings of vanadium at the P/V ratio of 1.1. Different characterization techniques like, BET, XRD, TEM, XPS and TPR have been used for the study. The surface areas of the different samples were slightly lower than the bare support. XRD revealed that crystalline V-P-O modifications were absent. TEM combined with energy dispersive analysis of X-rays (EDAX) demonstrated that the precipitated V-P-O phase was very well dispersed and anchored to the surface of the support bodies. XPS confirmed these results and revealed that the dispersion had increased during exposure to a n-butane/air mixture. Furthermore, the dispersion was not affected by the initial valence state of vanadium. With XPS, however, it was established that the surface of the applied V-P-O phase was enriched with phosphate. The reactivity

analysis of butane oxidation also concluded that the phosphorous modification have pronounced effect on the selectivity to MA (maleic anhydride). At low conversions catalysts were more selective towards the MA whereas at high conversion levels the selectivity to $CO_x$ was fairly low.

Lisi et.al. [30] compared the $TiO_2$- and $SiO_2$-supported catalysts containing bulk-like $VOPO_4$ particles to that of $TiO_2$-supported highly dispersed $VOPO_4$ in the oxidative dehydrogenation of ethane. XRD patterns revealed that the bulk-like VOP structures were formed for above monolayer catalyst (40-VOP/Ti). In contrast XRD pattern of monolayer catalyst (9-VOP/Ti) revealed only signals of the support, indicating a good dispersion of the active phase as also confirmed by the unchanged value of the original surface area of the $TiO_2$. The TPR study suggested that the vanadium is completely reduced to $V^{3+}$ by $H_2$ in a single step as observed for supported $V_2O_5$ catalysts in about the same range of temperature, the H/V ratio values were observed to be less than 2 for all the catalysts, the presence of $V^{+4}$ and $V^{+5}$ were proposed. Catalytic runs revealed that unsupported VOP exhibits a lower catalytic activity with high selectivity. At low temperatures the 40-VOP/Ti was more selective than the 9-VOP/Ti whereas at higher temperatures an opposite trend was observed as 9-VOP/Ti became more selective than the 40-VOP/Ti. They reported that the monolayer dispersion of $VOPO_4$ on a suitable support provides enhanced vanadium reducibility related to a great increase of activity in the ODH of ethane. $TiO_2$ was the support giving the best results. The deep modification of the active phase induced by the strong interaction with the support also affects the dependence of ethylene selectivity on the reaction temperature. Supports inhibiting dispersion, such as $SiO_2$ or $VOPO_4$ loading far exceeding the monolayer coverage, promote the formation of

bulk-like $VOPO_4$ aggregates showing a lower reducibility and poorer catalytic performances.

Deo and Wachs [20] studied the effect of additives on the structure and reactivity of $V_2O_5/TiO_2$ catalyst by Raman spectroscopy and methanol oxidation. Raman spectroscopy revealed that there are two type of interaction between additives and vanadium oxide phase. Noninteracting additives ($WO_3$, $Nb_2O_3$ and $SiO_2$) have no significant effect on the structure and surface vanadium oxide phase and no change was observed in the methanol activity and selectivity. For noninteracting samples the order of impregnation is not so important whereas for interacting samples ($K_2O$ and $P_2O_5$), order of impregnation have a pronounced effect on the structure and methanol activity of the surface vanadium oxide phase. The gradual addition of $K_2O$ or $P_2O_5$ to the $V_2O_5/TiO_2$ samples results in the decrease of methanol oxidation activity due to poisoning of surface vanadium oxide sites. When $P_2O_5$ is added to a previously prepared $V_2O_5/TiO_2$, however, a new vanadium phosphate compound observed by Raman spectroscopy, which was responsible for the increase in the di methyl ether selectivity.

Ciambelli et al. [29] have investigated the effect of iron substitution on bulk and $TiO_2$-supported $VOPO_4.2H_2O$ on the catalytic performances in ODH of ethane. The various characterization techniques, XRD, BET measurements, TPR and ammonia TPD experiments had been used. A uniform dispersion of the active phase was observed on the support structure. Both iron substitution and dispersion on $TiO_2$ appeared to significantly modify the redox and acid properties of vanadyl orthophosphate. A good correlation between the acid and redox properties of the catalysts and their catalytic performances

was also observed. For all the catalysts the conversion to $C_2H_6$ and the selectivity to $C_2H_4$ decrease and the selectivity to CO increase by increasing the contact time.

Savary et al. [31] tested the $VPO/TiO_2$ catalyst in the ODH of propane between 300 and 400 $^0$C and satisfactory performance ( upto 80 % of propene selectivity at 2 % of propane conversion at 300 $^0$C or 56 % of propene selectivity at 9% of propane conversion at 400 $^0$C) had been observed. The IR spectroscopic observations were performed under catalytic conditions with pyridine as a probe molecule to show the effect of water addition in the ODH of propane. These results clearly showed that $CO_x$ formation is linked to Lewis sites whereas Brönsted sites appear to be rather linked to propene formation.

Ciambelli et al. [32] also examined the titania supported VOP catalysts as a function of various loadings of VOP for the oxidative dehydrogenation of ethane. XRD, EDAX and SEM analysis and BET surface area measurements indicated that vanadyl phosphate is highly dispersed on the support up to monolayer coverage. A less homogeneous dispersion was observed for the above monolayer coverage sample. Thermogravimetric (TG) analysis suggested that the OH surface density of the supported materials are lower than that of $TiO_2$ and decreases with an increase in VOP content indicating that an interaction occurs between VOP and OH surface groups of $TiO_2$. A fraction of vanadium was present as V (IV) in the calcined samples as evaluated by EPR and TPR techniques. For monolayer catalyst the $V^{4+}$ was present in the form of $VO^{2+}$ hydrated species and similar magnetic parameters for all the catalysts suggested that the formation of a $VO(H_2O)^{2+}$-O-P bond in the material. The TPR experiments revealed that the extent of reduction increased when VOP was supported and the reducibility of the

catalyst was constant upto monolayer coverage and decreased when the monolayer coverage was exceeded. Both reducibility and acidity of vanadium phosphate was strongly enhanced by deposition on $TiO_2$ with respect to the bulk phase, as shown by TPR and $NH_3$ TPD technique, respectively. Ethylene selectivity decreases with the contact time as the ethylene is further oxidized to carbon oxides. The ethylene selectivity, however, increases with the temperature and this effect is attributed to the formation of V(IV), that is favored at increasing temperature.

## 2.4 Reaction mechanism

Chaar et. al. [36] studied the mechanism for ODH of propane and butane on V-Mg-O catalyst. They found that the reaction rate was independent of oxygen partial pressure for both propane and butane at 813 K. The reaction order with respect to alkane was 0.6 (±0.15) for propane and 0.85 (± 0.15) for butane. They concluded that the rate limiting step in ODH reaction was abstraction of a hydrogen atom from the alkane, resulting in the formation of an alkyl radical, which is followed by an abstraction of a second hydrogen atom to form alkenes.

Creaser and Andersson [37] have undertaken a detailed kinetic investigation of ODH on V-Mg-O catalyst. Various rate expressions are derived in order to fit the data based on Power Law type models and mechanistic models, such as, Langmuir-Hinshelwood and Mars-Van-Krevelen models. In these models, they have considered carbon oxides as secondary products. However, in a later study Creaser *et al.* [18] have concluded that the reaction data is best explained by considering carbon oxides as primary and secondary combustion products. Furthermore, they have proposed involvement of lattice oxygen in the ODH reactions.

Matra [38] investigated the surface properties of a series of $V_2O_5$ catalysts supported on different oxide supports by various characterization techniques. The surface vanadia species are found to be widely spread on the surface of $Al_2O_3$, zeolite and MgO, where as, on $TiO_2$ and $ZrO_2$ they are assembled in a layer almost completely covering the support. Furthermore, presence of V-OH Bronsted acid sites close to the active centers were detected. Based on the reaction and characterization studies they proposed that the propene molecules could be adsorbed on the Bronsted acid centers, the propene molecules then undergoes an over-oxidation by reaction with redox centers in the neighborhood.

Chen *et al.* [39] investigated the structure and catalytic properties of supported vanadium oxides for ODH reactions. The authors reported that the composition of the support influences the speciation of VOx species into monovanadates, polyvanadates and $V_2O_5$ clusters. Consequently, the catalytic behavior of supported vanadium oxide for ODH reactions changes. The ratios of rate coefficients and structural modifications caused by changes in VOx surface density or support composition was observed. Based on the above observations the authors suggested that sites required for ODH also catalyze the undesired combustion of propene.

Smits [40] studied the kinetics of the ODH on vanadia dopped niobia catalyst. The first step during the ODH of propane occurs between the oxygen species, which is most likely monatomic, and propane molecules. Furthermore, carbon oxides are primary and secondary combustion products and $CO_2$ is not formed from CO.

## 2.5 Kinetic modeling

Kinetic modeling provides us fundamental understanding regarding structure reactivity relationship of metal oxide catalysts and involves choice of a particular reaction mechanism and kinetic-parameter estimation of the same. Estimation of kinetic-parameters assists in the understanding of the reaction, operating the reactor under optimum conditions and for catalyst design.

Parameter estimation using traditional methods, such as, Levenberg-Marquardt's methods dependent strongly on initial guesses values. On the other hand, objective functions based on non-linear models are common features in most recent parameter estimation problems. These nonlinear models using experimental data generally contain more than one minimum for which tedious algorithms are required. These algorithms are sometimes susceptible to non-global optima. Thus, there is a need for development of efficient algorithms to replace the traditional methods. Recently, genetic algorithm has been effectively used for the estimation of reaction parameters. It shows promising results in terms of its accuracy and efficiency. Some information about GA in general is given elsewhere.

In an attempt to find initial estimates of rate constants for non-linear chemical kinetics, Wolf *et al.* [41] exploited GA techniques, without a priori assumption of rate determining step, in order to apply a wide range of operating conditions. Elliot *et al.* [42] used an inversion procedure of genetic algorithm to estimate rate parameters corresponding to product species measurement data from combustion of fuel experiments. This study suggests that its wide application to other chemical kinetics and optimization of other higher order kinetics is possible.

Park and Froment [43] estimated the kinetic parameter for the ethanol dehydrogenation reaction by using a hybrid genetic algorithm. Kinetic parameters were estimated over a wide range of space. They proposed that genetic algorithm provides a higher potential for accessing the global minima, where the most conventional methods are not much useful, mainly due to lack of good initial guess. It was observed that the performance of genetic algorithm strongly depends on the genetic algorithm running parameters. However, hybrid genetic algorithm is accurate and efficient regardless of running parameters of genetic algorithm.

Though attempts have been made to find out the reaction kinetics for different types of reactions, selection of objective function for multi-response nonlinear system has always been a matter of contention. Box and Drapper [44] have proposed that for multiresponse systems, in the absence of variance-covariance matrix, minimization of a determinant is the ideal objective function. The determinant contains the difference between the expected and predicted responses and error terms. They have added that the least square minimization should be used only when the variance-covariance matrix is known.

Boag et al. [45] have used the minimization of the determinant as the objective function for a multiresponse nonlinear system for the oxidation of *o*-xylene by vanadia catalyst. The minimization of the determinant was achieved by using Powell's method. Vajda and Valko [46] have proposed that for multiresponse problems minimization of the determinant is the objective function. However, they have observed that least square minimization can be used to obtain good initial guess or starting point for obtaining the final parameters, which involves minimization of determinant. Mezaki and Butt [47] have

compared the efficacy of two objective functions, minimization of determinant and nonlinear least square, for multivariate systems. They have shown that minimization of determinant scores over the nonlinear least squares for very complicated cases. They have shown that least square minimization can be used in absence of correlation between responses; otherwise the minimization of determinant provides the best estimate of parameters from multiresponse data.

Sulay [48] has used GA to analyze the effect of supported monolayer vanadia on titania and alumina and obtained promising results. However, the objective function used in that work is not amenable for multi-response systems. In this study it is observed that power law models better explain the data.

Recently, Routray et al. [49] have successfully implemented the determinant criterion and GA for determinig kinetic-parameters. The kinetic-parameters are further tested by using a profiling technique [50].

## 2.6 Genetic Algorithm (GA)

Genetic algorithm is an adaptive and learning-from-experience search technique based on the principles and mechanisms of natural selection and evolution [51-53]. Due to this the stronger individuals are likely to be the winners in a competing environments. GA's have received considerable attention for their potential as an optimization technique that can effectively search in the bounds of the complex problems. Though GA's may appear randomized they differ from simple random walk methods since historical information is effectively used for deciding new search points. The genetic algorithm operates in an iterative way on a fixed size pool of candidate solutions of the objective function to be

optimized. This pool of candidate solutions is analogous to the chromosomes of biological systems.

Initially, a population of solution is randomly generated. Each chromosome represents a possible solution for the given objective function to be optimized. The chromosome is represented by a string of binary bits (zero and ones) and is made up of a string of genes. These chromosomes can also be represented in terms of real codes. Each string would represent an independent variable representing the parameters θ. All these parameters are concatenated to form a bigger chain or chromosome. Each chromosome has a particular fitness value, which is associated with the objective function. These chromosomes evolve through successive iteration, called generations.

To create the next generation, all the chromosomes are either merged using a crossover operator, or modified using a mutation operator to form new chromosomes. Thus, a new generation is formed by selecting some parents and some off spring chromosomes and rejecting the weaker ones. This selection and rejection is done on the basis of fitness values. Those chromosomes having highest fitness values possess the highest chances of being selected as parents chromosomes. This process is repeated until a terminating condition is reached. The terminating condition used in the present study is the number of generations. To facilitate the GA evolution cycle, three fundamental operators are required. These operators are selection, crossover and mutation.

(i) **Selection:** Tournament selection is used in the present study. In this operation two chromosomes are randomly chosen from the population and the one with the higher fitness value is selected. This process is repeated until the new offspring pool is full.

(ii) **Crossover:** Crossover strategy determines how the parent chromosomes are combined to generate new off springs. Crossover is applied to randomly selected pairs of parents with a probability equal to a specified crossover rate. In the present study the crossover is 0.95.

(iii) **Mutation:** The main role of mutation is to provide genes not present in the initial population so as to prevent stagnation at local optima. If mutation rate is too low, then many genes are never being tried and if it is too high then, due to large perturbations, the offspring lose their resemblances to the parents. Consequently, GA does not learn from experience.

## 2.7 Summary

From the above review, it is clear that supported vanadium oxides are promising catalysts for the propane ODH reaction. The literature review of the characterization and reaction studies for the supported and unsupported VPO catalysts reveal that deep modification of the active vanadium phase occurs, which is induced by the strong interaction with the support. Acid-base and redox properties of the catalyst are critical parameters in deciding the intensity of modification and reactivity of modified catalytic samples. Changes in the reactivity of the phosphorous-modified VTi catalysts, however, have not been kinetically analyzed. Kinetic-analysis of the phosphorous-modified system is possible by kinetic-parameter estimation. Kinetic-parameters are effectively determined by applying GA as an optimization technique and using determinant as the objective function.

# Chapter: 3

## *EXPERIMENTAL DETAILS*

### 3.1 Sample Preparation

The unmodified and phosphorous modified titania supported vanadium oxide catalysts were prepared by the incipient wetness impregnation method. The incipient wetness volume of water for the $TiO_2$ support corresponds to 0.9 c.c. /g. The precursors used for vanadium and phosphorous were ammonium metavanadate ($NH_4VO_3$) and diammonium hydrogen phosphate [$(NH_4)_2HPO_4$], respectively. Initially, a large batch of the support was pretreated with an incipient volume of oxalic acid solution of a known concentration (0.1g/c.c.). The support was then dried in a desiccator at room temperature for 12 h, followed by drying at 383 K in an oven for 12 and finally calcined in an electric furnace at 733 K for 12 h.

The incipient wetness impregnation of vanadium and/or phosphorous of the above pretreated support was carried out with a solution containing the corresponding ions. For making the solution a vanadium oxalate solution was initially prepared by adding known amounts of ammonium metavanadate with stoichiometric amount of oxalic acid in water. For preparing the phosphorous modified samples required amounts of diammonium hydrogen phosphate was added to the above solution and stirred in water until the entire solid was dissolved. A deep blue solution was formed with and without phosphorous precursor, which was further diluted with double distilled water such that the total volume corresponds to the incipient wetness impregnation volume of the support. In a crucible the above solution was intimately mixed with the pretreated support to form a

paste. A similar procedure is followed for preparing titania supported vanadium and titania supported phosphorous oxide catalysts. For these systems only vanadium oxalate or di ammonium hydrogen phosphate solution was used. The paste was heat treated similar to that mentioned above for the pretreatment of the support.

In the present study 6 catalyst samples were prepared from the same pretreated support $TiO_2$ support and are given in Table 3.1 in terms of their nomenclature and wt % of $V_2O_5$ and $P_2O_5$. Sample 1 contained 3 wt % vanadium oxide as $V_2O_5$ and is referred to as 3VTi. Sample 2 contained 3 wt% $V_2O_5$ and 1.2 wt % $P_2O_5$. Similarly, samples 3 and 4 contained 2.9 wt % $V_2O_5$ and 2.3 wt % $P_2O_5$, and 2.9 wt % $V_2O_5$ and 4.5 wt % $P_2O_5$ , respectively. Sample 5 and 6 contained 1.2, and 4.6 wt % $P_2O_5$, respectively and are referred to as 1.2PTi and 4.6PTi. The nomenclature of the phosphorous-modified supported catalysts was based on the molar ratio of vanadium and phosphorous. For example, xVyPTi contains vanadium and phosphorous in a molar ratio of x: y on the $TiO_2$ support.

Unsupported vanadium-phosphorous samples in the same molar ratio mentioned in Table 3.1 were also prepared. For making the unsupported $V_2O_5$ sample, a vanadium oxalate solution was prepared by adding known amounts of ammonium metavanadate with stoichiometric amount of oxalic acid in water. The vanadium oxalate solution was heat treated to precipitate the solid. For preparing the VPO samples required amounts of diammonium hydrogen phosphate was added to a solution containing known amounts of vanadium oxalate (for maintaining a particular V: P ratio) and stirred in water until the entire solid was dissolved. A deep blue solution was formed, and this solution is further diluted with the same amount of water that is used in the preparation of supported

samples. The amount used for all the precursors are same as the amounts used in the preparation of supported catalysts. These solutions are then heat treated to co-precipitate the vanadium-phosphorous phase.

## 3.2 Characterization

The phosphorous-modified and unmodified VTi samples are characterized by determining their surface area and studying the XRD patterns, EPR spectra and TPR profiles.

### *i. Surface Area Studies*

The surface area of the catalyst samples were determined by a **COULTER SA 3100** analyzer equipped with **SA-VIEW** $^{TM}$ software using $N_2$ as the adsorbate. The **Gas Sorption** method using the BET equation was used by the analyzer.

### *ii. X-Ray Diffraction (XRD) Studies*

The XRD patterns were obtained in the range 10 to 50 $^0$ with a scanning rate of 10 $^0$ $min^{-1}$ on a **180 Debye flex-2002 X -ray diffractometer** equipped with a monochromator Ni filtered $K_\alpha$ radiation from a Cu target ($\lambda$= 1.54056 A°) was used.

### *iii. Electron Paramagnetic Resonance (EPR) Studies*

The EPR studies were performed on a BRUKER EMX 1444 EPR band spectrometer. The spectra were obtained under ambient conditions using a microwave frequency of ~ 9.86 GHz and a microwave power of 0.20 mW. The sweep time was 5.24 s and the magnetic field modulation frequency used was 100 kHz with modulation amplitude of 10 G. The values of receiver gain and time

constants were 1.0E04 and 0.64 ms, respectively. The EPR spectra were calibrated with DPPH using a duel cell.

### *iv. Temperature Programmed Reduction (TPR) Studies*

The TPR experiments were performed in a **Micromeritics Pulse Chemisorb 2705** apparatus. For this purpose 0.05 g of sample was taken in a quartz reactor. The pretreatment was performed by heating the sample in a He gas flow (30 cc/min) up to 423 K and then maintaining this temperature for 30 min. After cooling to 308 K, the sample was subsequently contacted with a $H_2$/Ar mixture ($H_2$/Ar volume ratio of 05:95 and total flow rate 50cc/min) and heated to a final temperature of 1230 K at a constant rate of 10 K/min. The hydrogen concentration of the exit gas was detected by a thermal conductivity detector.

## 3.3 Propane ODH Reactivity Studies

### *i. Reaction Setup*

All the catalysts were tested for the ODH of propane in a fixed bed, down flow, tubular quartz reactor of length 300 mm, inlet diameter of 10 mm and outlet diameter of 5 mm. A schematic of the reactor set-up is given in Fig. 3.1. The amount of catalyst was varied from 0.03 to 0.2g depending on the specific objective. Quartz powder was used as a diluent with the catalysts to prevent temperature gradients and to avoid channeling of gas within the catalyst bed. The catalyst bed containing the catalyst and quartz powder mixture was placed on the quartz wool at the center of the 300 mm long quartz reactor. The reactant mixture of $C_3H_8$ and air at a specified $C_3H_8$:$O_2$ molar ratio and a specified total flow rate were

controlled by two thermal mass flow controllers [**Bronkhost Hi-Tech, Model F201d FAC-22-V**]. The reaction temperature was controlled by a Chromel-Alumel thermocouple positioned just above the catalyst bed. This thermocouple was the sensor in a feedback control loop, containing a PID controller [**Fuji PXZ-4**] capable of controlling the reactor temperature within $\pm 1\ ^0$ C of the set point.

Product gas analysis was performed using an online **NUCON 5765** gas chromatograph (GC) possessing an **Hysep Q** column for separation of hydrocarbons, CO and $CO_2$. Carbon oxides (CO and $CO_2$) were converted to methane by a methanizer prior to detection. The oven temperature was maintained at 323 K and the quantitative detection of the carbon containing compounds was achieved by a flame ionization detector (FID). Several runs were taken to ensure that steady state conditions were attained.

### ii. *Reaction Studies*

Reaction studies were carried out for ensuring the reproducibility of the data, for determining the effect of contact time, and for obtaining the data for kinetic parameter estimation. For all these studies, each run was repeated two times in order to ensure reproducibility.

#### a. Data for reproducibility studies

For this study two catalyst sample were chosen: 3VTi and 1V1PTi. For both the samples, the $C_3H_8$:$O_2$ molar ratio of propane to air was maintained at 1:1. The total volumetric flow rate was 75 cc/min. The weight of 3VTi and 1V1PTi catalysts were 0.05 and 0.10 g for the reproducibility studies. Initially, the temperature was increased from 613 to 673 K at 20 K intervals. Subsequently, the temperature was

reduced to 613 K at 20 K intervals. At each temperature the reaction data collected. Thus, the data was collected at 613, 633, 653, 673, 653, 633 and 613 K.

**b. Data for contact time effects**

For carrying out contact time studies over a particular catalyst at 643 K the total volumetric flow rates were varied as 120, 90, 75, 45, 30 and 20 cc/min. The $C_3H_8$:$O_2$ molar ratio was maintained at 2:1.

**c. Data for kinetic-parameter estimation**

To obtain the data for kinetic parameter estimation the $C_3H_8$: $O_2$ ratio was varied as 3:1, 2:1 and 1:1 and at each ratio the data was collected at 613, 633, 653 and 673 K. The total volumetric flow rate was maintained at 75 cc/min. The amount of catalyst used for the contact time studies and for the data used for the kinetic-parameter estimation are given in the second and third columns of Table 3.2.

## *iii. Reactivity Calculations*

Analyzed products of the ODH reaction were propene ($C_3H_6$), carbon monoxide (CO), carbon dioxide ($CO_2$) and unconverted propane ($C_3H_8$). Each of these components gave separate peaks in the chromatograph. Chromatogram peak areas were multiplied by corresponding sensitivity factors given by Dietz [54] to obtain true areas representative of the weight of each component. The values obtained were then converted to represent mole numbers of the components. Mole fractions were calculated based on the mole numbers. The inlet number of moles was multiplied by mole fraction of each component in the exit to obtain moles of components in the exit gas. The calculations of conversion, selectivity, yield and carbon balance were based on these mole fractions. For calculation purposes, the total number of moles of reactants was assumed to be unchanged. This

approach is justified since the conversion levels were low and nitrogen was used as a dilutant.

**a. Conversion**

The conversion was calculated as follows:

$$\text{Conversion}, \% = \frac{\text{Moles of Propane converted}}{\text{Moles of Propane in}} \times 100$$
$$= \frac{\text{Moles of Propane in - Moles of Propane out}}{\text{Moles of Propane in}} \times 100 \qquad (3.1)$$

**b. Selectivity**

Selectivity for the reactions leading to formation of a particular product ($C_3H_6$, CO and $CO_2$) was calculated as follows:

$$\text{Product selectivity}, \% = \frac{\text{Moles of Product formed}}{\sum \text{Moles of all Products formed}} \times 100 \qquad (3.2)$$

The denominator of eqn. 3.2 represents the moles of propane converted. The CO and $CO_2$ selectivity was based on the moles of propane converted to CO or $CO_2$, i.e. one mole of propane forms three moles of CO or $CO_2$.

**c. Yield**

The amount of propene formed was represented by yield, which was calculated as follows:

$$\text{Propene yield}, \% = \frac{\text{Moles of Propene formed}}{\text{Moles of Propane in}} \times 100 \qquad (3.3)$$

Equation 3.3 is essentially a product of Eqns.3.1 and 3.2.

**d. Carbon Balance**

Carbon balance represents the accuracy of measurements. Furthermore, it provides an indicator as to whether any carbon deposition occurs. Carbon balance calculations are based on the formula given in Eqn. 3.4.

$$\text{Carbon balance} = \frac{\text{Moles of Carbon in products}}{\text{Moles of Carbon in reactant}} \qquad (3.4)$$

## 3.4 Kinetic-Parameter Estimation

To obtain the kinetic parameters the reactor is subjected to integral analysis. Advantages of this method over conventional differential analysis are mentioned in detail elsewhere [33]. To proceed with kinetic parameter estimation the reactor is initially modeled.

### *i. Modeling of the reactor and problem formulation*

To model the reactor the following assumption were considered.

- The reactor operates under isothermal and steady state condition.
- Total number of moles of gases remains constant.
- There is no heat and mass transfer limitations.
- Gas phase reactions are negligible.
- Catalyst deactivation is within limits.

All assumptions are justified since propane conversions are low (<10 %) and nitrogen and quartz act as a dilutant.

The differential material balance equation for each component, i, for a particular reaction network can be written as

$$V_0 y_i |_W - V_0 y_i |_{W+dW} - \sum_j n_{ij} r_j dW = 0 \qquad i = 1.....v \qquad (3.5)$$

Where,

$V_0$ = volumetric flow rate of the feed

$y_i$ = mole fraction of the $i^{th}$ component.

$n_{ij}$ = stoichiometric coefficient of the $i^{th}$ component for the $j^{th}$ reaction

$r_j$ = rate of $j^{th}$ reaction and is a function of $K_j$ and $x_i$ or $r_j = f_j(x_i, K_j)$,

$K_j$ = kinetic parameters for the $j^{th}$ reaction

$v$ = number of components

$W$ = weight of the catalyst.

Simplification of the above equation with the assumptions mentioned above results in Eqn. 3.6.

$$\frac{dy_i}{dW} = \sum_j n_{ij} r_j \Big/ V_0 \qquad (3.6)$$

The set of ordinary differential equations represented in Eqn. 3.6 can be solved to obtain the output mole fraction of each component based on the initial value of component mole fraction, $y_{io}$ and knowledge of W, $n_{ij}$, $V_0$ and $r_j$. The output mole fraction is obtained by integrating over the entire mass using Runga-Kutta fourth order technique. The specific reaction rate, $r_j$, is dependent on values of kinetic-parameter, $\theta_j$, which are non-linear in nature and some or all mole fractions, $y_i$.

The response data, the output mole fraction of $C_3H_8$, $C_3H_6$, CO and $CO_2$ are assumed to be well described by a nonlinear model given by

$$Y_h = g_h(\theta, x) + Z_h, \qquad h = 1, 2, ...., v \qquad (3.7)$$

where,

$Y_h$ = vector of random variables representing the response variable

$g_h(\theta, x)$ = predicted concentration

θ = parameter vector

$x$ = concentration vector

$Z_h$ = error associated while calculating the response $h$

The predicted output mole fraction for the $i^{th}$ component and $u^{th}$ experiment $y_{iu,pred}$ obtained this way can then be compared with the actual output mole fraction $y_{iu}$. To obtain the best value of the parameters minimization of an objective function is required [51].

## *ii. Objective function*

When the variance and co-variances $\sigma_{ij}$ are known then the kinetic parameters are estimated by minimization of a multiresponse objective function criterion [55]. This is given in Eqn. 3.8.

$$\sum_{h=1}^{v}\sum_{k=1}^{v}\sigma^{hk}\sum_{u=1}^{n}[y_{hu}-\hat{y}_{hu}][y_{ku}-\hat{y}_{ku}] \qquad (3.8)$$

Where, $\sigma^{hk}$ are the elements of the $v$ x $v$ error covariance inverse matrix.

If the elements of the response vector are uncorrelated $\sigma_{hk} = 0, \text{for} h \neq k$ and further simplification of Equation 3.4 is possible. In this case, minimization of the equation 3.4 would correspond to standard weighted least square, using the reciprocals of the variances as the weight [44].

$$\sum_{h=1}^{v}\sum_{u=1}^{n}\frac{1}{\sigma_{hh}}(y_{hu}-\hat{y}_{hu})^2 \qquad (3.9)$$

Where $\sigma_{hk}$ is the element in the $h^{th}$ row and $k^{th}$ column of the $v$ x $v$ error covariance matrix.

For multiresponse systems and when responses are correlated, the ideal criterion is the minimization of the determinant is given below [44, 46-47 and 55-56].

Determinant criteria for multiresponse systems = min $|Z_{hk}|$

Where, $Z_{hk}=\sum_{u=1}^{n}(y_{hu}-g_{hu})(y_{ku}-g_{ku})$ , h and k = 1,..$v$ (3.10)

n = no. of experiments

$v$ = no. of responses

$y_{hu}$ = experimental mole fraction of $h^{th}$ component in $u^{th}$ experiment

$g_{hu}$ = predicted mole fraction of $h^{th}$ component in $u^{th}$ experiment

In the present study the determinant criteria given by equation 3.10 is considered.

### *iii. Genetic Algorithm (GA)*

Minimization of objective function is achieved by applying a Genetic Algorithm (GA). The GA source code is taken from the KANGAL lab, IIT Kanpur, and is developed by Deb and co-workers [57]. The GA implementation in this study is restricted to real coded variables only. All constraints used in this code is greater-than-equal-to type (g >= 0) and normalized. This general code is then modified according to the present study for obtaining the kinetic-parameters. Initially, a population of solution is randomly generated. The size of population was 120 to 200 for power law type models and 80 to 150 for MVK models. These two models are discussed later. The variable boundaries are fixed for each parameter and fixation of boundaries is done according to

previous knowledge of the parameters. Selection of parents from the pool of solutions is done by tournament selection. The size of tournament in the present study was 2. Crossover probability exchanges information among parent solutions whereas polynomial mutation operator is utilized to introduce the extra diversity to the solutions. The values of crossover and mutation probability were 0.9 and 0.1, respectively. In the present study the parameters are real, thus, simulated binary crossover (SBX) is considered. The exponents of SBX and mutation were 2 and 200 respectively. The termination criteria used in this GA code was the total number of generations. The number of generations was varied from 5000 to a maximum of 50000 to obtain stable solutions. All the parameters used in the GA code are listed in Table 3.3.

### *iv. Reaction Scheme*

The generalized reaction network for the ODH of propane is shown in Fig 3.2. The state of carbon atom is only considered in this reaction scheme. The generalized reaction can be represented by six reactions steps, $r_1$ to $r_6$. Propene is formed by the ODH of propane ($r_1$), which can degrade to form CO and $CO_2$ by reactions $r_2$ and $r_3$, respectively. The carbon oxides, CO and $CO_2$, can also be formed directly from propane by reactions $r_5$ and $r_4$, respectively. Furthermore, $CO_2$ can be formed by the oxidation of CO by reaction $r_6$.

The stoichiometric equations corresponding to each reaction in the reaction network is given in equations 3.11 to 3.16.

$$C_3H_8 + 0.5O_2 \rightarrow C_3H_6 + H_2 \qquad (3.11)$$

$$C_3H_6 + 3O_2 \rightarrow 3CO + 3H_2O \qquad (3.12)$$

$$C_3H_6 + 4.5O_2 \rightarrow 3CO_2 + 3H_2O \quad (3.13)$$

$$C_3H_8 + 5O_2 \rightarrow 3CO_2 + 4H_2O \quad (3.14)$$

$$C_3H_8 + 3.5\,O_2 \rightarrow 3CO + 4H_2O \quad (3.15)$$

$$CO + 0.5O_2 \rightarrow CO_2 \quad (3.16)$$

The stoichiometric coefficient, $n_{ij}$, used for the problem formulation is given by these equations.

## v. *Reaction Models*

Choice of the reaction model is important for kinetic analysis. For the purpose of understanding the structure-reactivity relationship for unmodified and phosphorous-modified VTi catalyst, power law and mechanistic type of models were considered in the present study. Two power law models, PL-1 and PL-2, were used to explain the reaction data obtained during propane ODH. Among the various mechanistic models present, a Mars van Kremelan (MVK) mechanism based on the PL-1 and PL-2 models were used.

### a.Power Law Models

In the power law models it is assumed that the reaction rate is proportional to the partial pressure of a reactant raised to an exponent. Based on the reactions given in equations 3.11 to 3.16, the reaction rates are given in equations 3.17 to 3.22.

$$r_1 = k_1 (P_{C_3H_8})^{a_1} (P_{O_2})^{b_1} \quad (3.17)$$

$$r_2 = k_2 (P_{C_3H_6})^{a_2} (P_{O_2})^{b_2} \quad (3.18)$$

$$r_3 = k_3 (P_{C_3H_6})^{a_3} (P_{O_2})^{b_3} \quad (3.19)$$

$$r_4 = k_4 (P_{C_3H_8})^{a_4} (P_{O_2})^{b_4} \quad (3.20)$$

$$r_5 = k_5 (P_{C_3H_8})^{a_5} (P_{O_2})^{b_5} \quad (3.21)$$

$$r_6 = k_6 (P_{CO})^{a_6} (P_{O_2})^{b_6} \quad (3.22)$$

Where,

$k_i$ = rate constant for reaction i, where i = 1,2,..,6, and

$a_i$ and $b_i$ = partial pressure exponent of the reactant for reaction i

The rate constants, $k_i$, consists of two parameters: the pre exponential factor, $k_{i0}$, and the activation energy, $E_i$. Thus, each reaction, $r_i$, contains four parameters in the power law models: $k_{i0}$, $E_i$, $a_i$ and $b_i$.

**1) PL-1 Model**

The PL-1 model assumes that CO and $CO_2$ are secondary products and are formed from propene. Thus, $r_1$, $r_2$ and $r_3$ are the only reactions considered. Consequently, there are 12 parameters in this model. This type of reaction scheme has been considered previously [12, 37].

**2) PL-2 Model**

The PL-2 model considers that CO and $CO_2$ are the primary products formed by reactions $r_4$ and $r_5$, respectively. Thus, propane reacts to form $C_3H_6$, CO and $CO_2$ through the reactions $r_1$, $r_4$ and $r_5$ only. Thus, there are 12 parameters in the PL-2 model also. The parameters involved in the PL-1 and PL-2 models are given in Table 3.4.

**b. Mechanistic Models**

Mechanistic models are based on the knowledge of the relationships between reactants and surface properties of the catalyst. To construct the mechanistic models a plausible mechanism must be known based on physical and chemical grounds. In the present study Mars-Van Krevelen (MVK) type reaction models have been used to explain the kinetics of the reaction. Two MVK models, MVK-1 and MVK-2, are formulated based on the PL-1 and PL-2 reaction model.

**1) MVK-1 Model**

According to this Mars-van Krevelen mechanism for the ODH reactions the alkane molecules react with lattice oxygen of the catalyst to produce alkene molecules and carbon oxides. The gas phase oxygen replenishes the lattice oxygen by the re-oxidation of the catalyst. Thus, there are four reactions considered $r_1$, $r_2$, $r_3$ and $r_4$ [49]. These four reactions are given below

1.Formation of propene ($r_1$):

The gas phase propane reacts with lattice oxygen forming gas phase propene.

$$C_3H_8(g)+O(s) \rightarrow C_3H_6(g)+H_2O+*_{red} \qquad (3.23)$$

Where $*_{red}$ is a reduced site.

2.Formation of CO from propene ($r_2$):

The gas phase propene reacts with lattice oxygen to form gas phase CO.

$$C_3H_6(g)+6O(s) \rightarrow 3CO(g)+3H_2O+6*_{red} \qquad (3.24)$$

3.Formation of $CO_2$ from propene ($r_3$):

The gas phase propene reacts with lattice oxygen forming $CO_2$ gas.

$$C_3H_6(g) + 9O(s) \rightarrow 3CO_2(g) + 3H_2O + 9*_{red} \quad (3.25)$$

4.Re-oxidation ($r_4$):

Finally, the catalyst is re-oxidized by gas phase oxygen.

$$O_2 + 2*_{red} \rightarrow 2O(s) \quad (3.26)$$

The reaction rate for the above four reactions, (3.27) to (3.30), are expressed as

$$r_1 = k_1 P_{C_3H_8}(1-\beta) \quad (3.27)$$

$$r_2 = k_2 P_{C_3H_6}(1-\beta) \quad (3.28)$$

$$r_3 = k_3 P_{C_3H_6}(1-\beta) \quad (3.29)$$

$$r_4 = k_4 P_{O_2}\beta \quad (3.30)$$

Where,

$k_j$ is the rate constant for the $j^{th}$ reaction, in ml STP $min^{-1}$ (g cat)$^{-1}$ $atm^{-1}$

$P_i$ is the partial pressure of the component, *i, in atm*

$\beta$ is the degree of reduction of the catalyst, which is dimensionless

Assuming that the rate of oxygen consumed in the reactions $r_1$, $r_2$ and $r_3$ is equal to the rate of oxygen replacement by the reaction $r_4$, $\beta$ can be expressed as

$$\beta = \frac{0.5k_1 P_{C_3H_8} + 3.0k_2 P_{C_3H_6} + 4.5k_3 P_{C_3H_6}}{0.5k_1 P_{C_3H_8} + 3.0k_2 P_{C_3H_6} + 4.5k_3 P_{C_3H_6} + k_4 P_{O_2}} \quad (3.31)$$

**2) MVK-2 Model**

The MVK-2 model differs from the MVK-1 model with regard to the formation of CO and $CO_2$. In the MVK-2 model, CO and $CO_2$ are directly formed from the gas phase propane only. Thus, there are four reactions considered, $r_1$, $r_2$, $r_3$ and $r_4$. The reaction $r_1$

and $r_4$ are similar to the MVK-1 model whereas $r_2$ and $r_3$ are different and given by Eqns. 3.32 and 3.33.

1.Formation of propene ($r_1$):

The gas phase propane reacts with lattice oxygen forming gas phase propene.

$$C_3H_8(g)+O(s) \rightarrow C_3H_6(g)+H_2O+*_{red} \quad (3.23)$$

Where $*_{red}$ is a reduced site.

2. Formation of CO from propane ($r_2$):

The gas phase propane reacts with lattice oxygen to form gas phase CO.

$$C_3H_8(g)+7O(s) \rightarrow 3CO(g)+4H_2O+7*_{red} \quad (3.32)$$

3. Formation of $CO_2$ from propane ($r_3$):

The gas phase propane reacts with lattice oxygen forming $CO_2$ gas.

$$C_3H_8(g)+10O(s) \rightarrow 3CO_2(g)+4H_2O+10*_{red} \quad (3.33)$$

4. Re-oxidation ($r_4$):

Finally, the catalyst is re-oxidized by gas phase oxygen.

$$O_2+2*_{red} \rightarrow 2O(s) \quad (3.26)$$

The reaction rate for the above four reactions, are expressed as

$$r_1 = k_1 P_{C_3H_8}(1-\beta) \quad (3.27)$$

$$r_2 = k_2 P_{C_3H_8}(1-\beta) \quad (3.34)$$

$$r_3 = k_3 P_{C_3H_8}(1-\beta) \quad (3.35)$$

$$r_4 = k_4 P_{O_2} \beta \tag{3.30}$$

Similar to equation 3.31, β for MVK-2 model is expressed as,

$$\beta = \frac{0.5k_1 P_{C_3H_8} + 3.5k_2 P_{C_3H_8} + 5.0k_3 P_{C_3H_8}}{0.5k_1 P_{C_3H_8} + 3.5k_2 P_{C_3H_8} + 5.0k_3 P_{C_3H_8} + k_4 P_{O_2}} \tag{3.36}$$

## *vi. Reparameterisation*

Parameter estimates obtained by fitting models to data are often highly correlated with each other. Under such circumstances the parameters are of little use for predicting the nature of the system. In chemical kinetics high correlations are frequently encountered between estimates of the parameters in the Arrhenius expression for a rate constant making the elucidation of a reaction network very difficult [58]. To decrease the correlation between parameters reparameterisation is required. Reparameterisation is achieved by reformulating the rate constants as

$$k_i = k_{io} \exp[\frac{-E_i}{RT}(\frac{1}{T} - \frac{1}{T_m})] \tag{3.37}$$

Where,

$k_{i0}$ = pre-exponential factor, units depend on the model type

$E_i$ =activation energy for the reaction i, kJ/mol

$T$ = actual reaction temperature, K

$R$ = universal gas constant, kJ/kmol K

$T_m$ = mean temperature, K

Furthermore, for power law models, PL-1 and PL-2, the partial pressure of a component, $P_j$, is also centered about the mean partial pressure of the component, i.e., $(\frac{P_j}{P_j^m})^{a_i}$.

Where,

$P_j^m$ = mean partial pressure of the component $j$, atm

This type of centering reduces the correlation between the exponent and pre-exponential factor [58, 59].

### *vii. Standard Error Calculation*

Standard error calculation provides the view of accuracy associated in the estimation of kinetic parameters. For standard error calculation, a Bayesian criterion was followed in which it was assumed that the each row of Z follows a multivariate normal distribution [60].

Accordingly, the standard error $se(\hat{\theta}_p)$ [60] for the kinetic-parameters, $\theta_p$, is then given by

$$se(\hat{\theta}_p)=\{(2s^2\Gamma^{-1})_{pp}\}^{0.5} \tag{3.38}$$

Where, $2s^2\Gamma^{-1}$ is the covariance matrix $\hat{\theta}$. The value of $s^2$ is obtained by dividing the determinant value at optimized conditions with the degrees of freedom N-P, where N is the number of experiments and P is the number of kinetic parameters. Furthermore, $\Gamma$ is an approximate Hessian of $|Z^TZ|$ calculated at the optimized kinetic-parameter values.

**Table 3.1: Nomenclature and composition of the samples**

| Sl. No. | Nomenclature | wt % of $V_2O_5$ in the sample | wt % of $P_2O_5$ in the sample | V: P molar ratio |
|---|---|---|---|---|
| 1 | $TiO_2$ | 0.0 | 0.0 | -- |
| 2 | 3VTi | 3.0 | 0.0 | -- |
| 3 | 2V1PTi | 3.0 | 1.2 | 2:1 |
| 4 | 1V1PTi | 2.9 | 2.3 | 1:1 |
| 5 | 1V2PTi | 2.9 | 4.5 | 1:2 |
| 6 | 1.2PTi | 0.0 | 1.2 | -- |
| 7 | 4.6PTi | 0.0 | 4.6 | -- |

**Table 3.2: Different weights of catalysts used during reaction studies**

| Catalyst Nomenclature | Weight (g) | |
|---|---|---|
| | Contact Time Studies | Data for Kinetic-Parameter Estimation |
| 3VTi | 0.05 | 0.03 |
| 2V1PTi | 0.05 | 0.04 |
| 1V1PTi | 0.10 | 0.10 |
| 1V2PTi | 0.20 | 0.20 |

**Table 3.3: GA parameters used in the present study**

| GA Parameters | Values | |
|---|---|---|
| | **Power Law Models** | **MVK Models** |
| Generations | 5000 to 50000 | 5000 to 50000 |
| Population size | 120 to 200 | 80 to150 |
| Crossover probability | 0.9 | 0.9 |
| Mutation probability | 0.1 | 0.1 |
| Tournament size | 2 | 2 |
| Exponent for simulated binary crossover | 2 | 2 |
| Exponent for mutation | 200 | 200 |
| Seed Value | 0.123 to 0.2 | 0.123 to 0.2 |

**Table 3.4 Contributing reactions as per Figures 3.3 and 3.4 and corresponding number of kinetic parameters for the PL-1 and PL-2 model.**

| Kinetic Model | Contributing Rates | Number of Parameters | | | | |
|---|---|---|---|---|---|---|
| | | $k_{io}$ | $E_i$ | $a_i$ | $b_i$ | Total |
| PL-1 | $r_1$ , $r_2$, $r_3$. | 3 | 3 | 3 | 3 | 12 |
| PL-2 | $r_1$, $r_4$, $r_5$ | 3 | 3 | 3 | 3 | 12 |

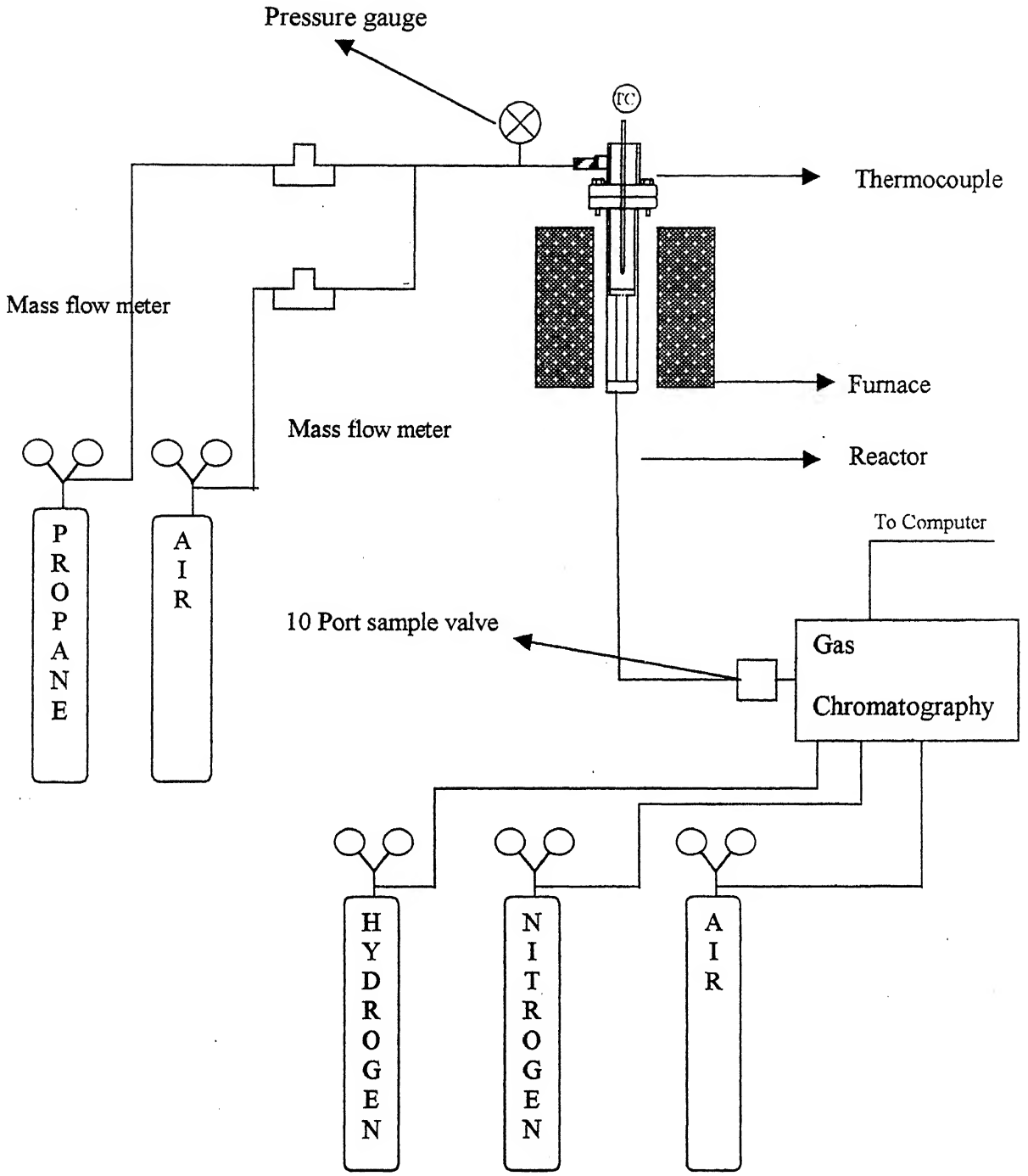


**Figure 3.1 Reactor setup**

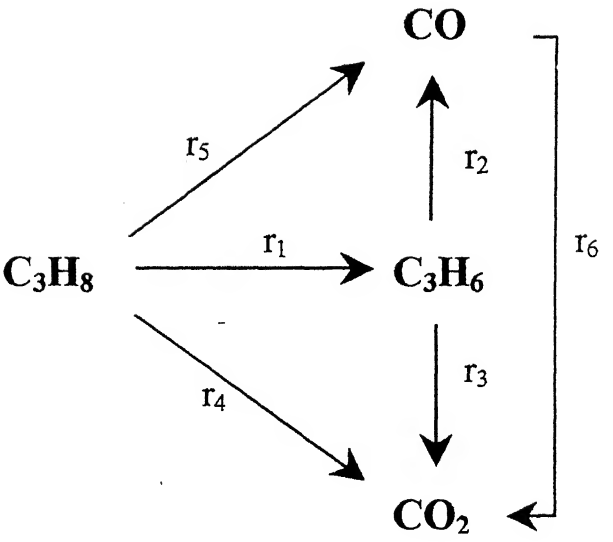


**Figure 3.2 Generalized reaction scheme for propane ODH**

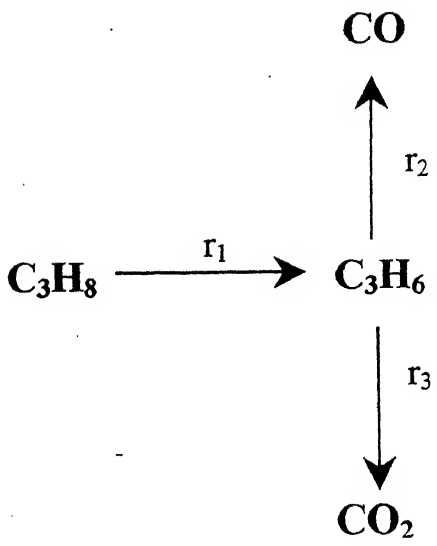


**Figure 3.3 The PL-1 power-law model**

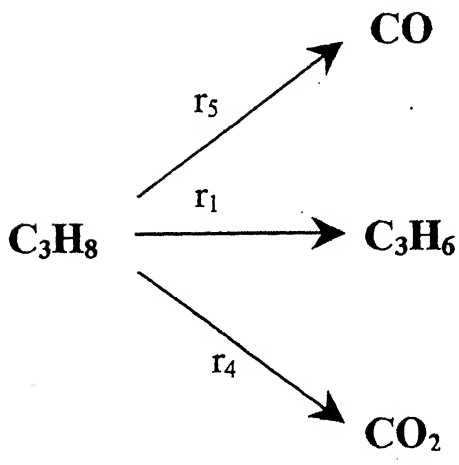


**Figure 3.4 The PL-2 power-law model**

# Chapter: 4

## *RESULTS & DISCUSSION*

Three phosphorous-modified and one unmodified $V_2O_5/TiO_2$ catalysts were prepared with various vanadium to phosphorous ratios. Two $P_2O_5/TiO_2$ catalysts were also prepared. These samples were analyzed for their surface area and by XRD, TPR and EPR techniques. The characterized samples were then studied for the propane ODH reaction. Initially, the results of the characterized samples are presented, which are followed by the results of the propane ODH reaction.

## *4.1 Characterization Studies*

### *i. Surface Area Studies*

The surface areas of pure titania ($TiO_2$), $3\%V_2O_5/TiO_2$, phosphorous modified $V_2O_5/TiO_2$ and two $P_2O_5/TiO_2$ samples were obtained by applying the BET equation and are tabulated in the third column of Table 4.1. Also given in Table 4.1 are the $T_{max}$ and H/V ratios, which are discussed later. The surface area values for all the samples are between 41 and 47 $m^2/g$ and appear to be constant. Consequently, it appears that the support is not affected significantly during preparation of the catalysts. Others have observed similar variations in surface area [26, 29, 30, 32].

### *ii. X-Ray Diffraction Studies*

The XRD patterns of pure $TiO_2$, and the six titania supported samples are shown in Fig.4.1. In Fig. 4.1 the intensity is plotted versus the 2θ value. For all the samples major

peaks were observed at 25.33 and 48.13 $^0$ with minor peaks at 26.98, 28.62, 36.24 and 38.82 $^0$. These peaks correspond to the $TiO_2$ only and suggest that the support is unaffected. Similar XRD patterns are reported in the literature [26, 29, 30, 32].

The XRD pattern of unsupported $V_2O_5$ in Fig.4.2 reveals that major peaks are present at 20.33, 21.76, 26.24, 31.06 and 32.44 $^0$ and minor peaks at 34.35, 41.29 and 47.39 $^0$. Comparison of the XRD spectra suggests that peaks due to bulk $V_2O_5$ are absent in 3VTi and the phosphorous-modified VTi samples. Furthermore, the XRD patterns in Fig. 4.2 reveal that unsupported 2V1P possesses major peaks at 12.27, 20.36, 26.33 and 29.00 $^0$ and minor peaks at 31.12 and 41.23 $^0$; unsupported 1V1P possesses major peaks at 12.12 and 28.91 $^0$ and minor peaks at 18.74, 24.12 and 31.38 $^0$; and unsupported 1V2P possesses major peak at 22.91 and 36.50 $^0$ and minor peaks between 25.56 and 28.65 $^0$. From Fig. 4.2 it appears that some bulk $V_2O_5$ is present in the 2V1P sample. The XRD pattern for the 1V1P and 1V2P samples, howevere, does not show the presence of any bulk $V_2O_5$. The other peaks in the XRD pattern of 2V1P, 1V1P and 1V2P correspond to different VPO phases. Comparison of the XRD patterns for the unsupported and supported phosphorous-modified vanadia samples suggests that amorphous or XRD transparent phases are present in the phosphorous-modified VTi samples. The $P_2O_5/TiO_2$ and the unsupported vanadium-phosphorous samples were not considered for further characterization since no additional information about the supported VPO phase was obtained.

### *iii. Electron Paramagnetic Resonance Studies*

The EPR spectra of the unmodified and phosphorous-modified VTi samples are shown in Fig. 4.3. The spectra are centered at 3400 G with a sweep width of 2000 G. For all the

samples a strong axially symmetric peak was observed with a g-value = 2.00 due to a hydrated $VO^{2+}$ species. The intensity of peaks increases with phosphorous content in the samples. The intensity was maximum for the 1V2PTi sample, whereas the least intensity was observed for the 3VTi sample. Broadness of peaks also followed similar behavior since the ΔG values increased with phosphorous content. The spectra of 2V1PTi and 1V1PTi are similar and different from the 3VTi and 1V2PTi spectra suggesting that similar paramagnetic species are present in the 2V1PTi and 1V1PTi samples. Similar EPR spectra have also been observed previously [28, 32, 61].

After calcination the vanadium is mainly in the form of $V^{5+}$ species. The EPR spectra suggests that small amounts of $V^{+4}$ species are also present. The axially symmetric signals reveal the chemical equivalence and magnetic dilution of isolated $V^{4+}$ ions that are dispersed in a $V^{5+}$ network as hydrated $VO^{2+}$ species. Similar spectrum of phosphorous-modified VTi samples suggest the formation of $VO(H_2O)^{2+}$-O-P species in the material. [28, 32].

### *iv. Temperature Programmed Reduction Studies*

TPR studies were performed for the phosphorous-modified and unmodified VTi samples and the TPR profiles are shown in Fig. 4.4. The TPR profiles of the $TiO_2$ support did not show any features in the temperature range considered and is not shown for convenience. A single $T_{max}$ is observed in Fig. 4.4 for all samples except for 1V2PTi where two reduction peaks are observed. Thus, it appears that a different species is formed in the 1V2PTi samples. The $T_{max}$ temperatures for the four samples are reported in the fourth column of Table 4.1. From the data presented in Table 4.1 it is observed that the $T_{max}$ temperature of the first reduction peak gradually increases with an increase in

phosphorous content in the samples. The $T_{max}$ temperature for the2V1PTI, and 1V1PTi appear to be similar. A single broad reduction peak is observed for 1.2PTi at 820 K and is not shown in Fig. 4.4 for convenience.



For quantitative analysis, the reduction peak areas were integrated to determine the amount of hydrogen consumed. The hydrogen consumed per vanadium atom present in the sample is determined and the H/V atomic ratio calculated. The H/V values are reported in the fifth column of Table 4.1. It is observed that the H/V atomic ratio is 2.0 for 3VTi indicating the reduction of $V^{+5}$ to $V^{+3}$. The H/V value decreases with an increase in phosphorous content for the modified catalysts since the H/V atomic ratios for 2V1PTi, 1V1PTi, and 1V2PTi are 1.6, 1.4 and 1.3, respectively. Similar TPR results showing the affect of phosphorous modification have also been observed before [26, 31].

The higher $T_{max}$ values with an increase in phosphorous content suggest that the vanadia sites are less reducible. Furthermore, the H/V ratio ranging from 1.3 to 1.6 for the phosphorous-modified VTi samples suggest the presence of both $V^{5+}$ and $V^{4+}$ in the fresh samples. The presence of $V^{4+}$ is in agreement with the results of EPR analysis. Additionally, the decrease in the H/V ratio suggests a lesser amount of $V^{+5}$ species is present. Indeed the EPR spectra shows an increase in $V^{+4}$ species that corresponds to a decrease in $V^{5+}$ species.

Thus, surface vanadium oxide species are formed on the $TiO_2$ support that are primarily in the $V^{5+}$ oxidation state. Phosphorous-modification of the 3VTi sample results in the formation of some hydrated $V^{4+}$ species. A new reducible phase is obtained for the sample containing vanadium to phosphorous in a ratio of 1:2. The reducibility of the

surface vanadia species decreases with phosphorous modification. Finally, deposition of vanadia and phosphorous-vanadia on the support does not affect the vanadia structure.

## *4.2 Reactivity Studies*

The propane ODH reaction over the 3VTi, 2V1PTi, 1V1PTi and 1V2PTi were carried out to obtain data for the reproducibility studies, contact time effects and data for kinetic-parameter estimation. Blank runs were also taken to ensure that homogeneous reaction does not occur. Under the operating conditions employed the $TiO_2$ support, 1.2PTi and 4.6PTi were inactive for the ODH of propane. The raw areas obtained from the experiments carried out over phosphorous-modified and unmodified VTi catalysts are given in the Appendix. As mentioned previously the raw data was used to calculate the mole fraction, conversion, selectivity and yield.

### *i. Data for Reproducibility Studies*

Two catalyst unmodified 3VTi and the modified 1V1PTi catalyst were chosen to determine the reproducibility of the reaction data. Results obtained in these studies are shown in Figs. 4.7 and 4.8. In these figures the $C_3H_6$, CO and $CO_2$ yields were plotted as the temperature was initially increased and then decreased. Arrows show the temperature trends. From Figs. 4.7 and 4.8 it is observed that the yields are essentially independent of the temperature history. Consequently, the reaction data appears reproducible in the operating-conditions considered in the present study.

### *ii. Data for Contact Time Studies*

To analyze the effect of contact time the propane ODH reaction were performed over the four ODH active catalyst samples for different contact times at 643 K and $C_3H_8$:$O_2$ ratio

of 2:1. The results of these runs are shown in Fig. 4.5 and 4.6. In Fig. 4.5 the propane conversion is plotted versus contact time for unmodified and phosphorous-modified VTi catalysts and it is observed that the conversion increases with an increase in contact time. Furthermore, it is clear from Fig. 4.5 that at the same contact time the conversion decreased with an increase in phosphorous content in the catalyst. For example, at a contact time of 67 (Kg $m^{-3}s$) the conversion for 3VTi was the highest, 2.3 %, followed by 2V1PTi, 1.7 %, 1V1PTi, 1.1 % and finally 1V2PTi, 0.5 %. Thus, in terms of activity 3VTi > 2V1PTi > 1V1PTi > 1V2PTi.

In Fig. 4.6 the propene selectivity is plotted versus the propane conversion for the different catalysts. Figure 4.6 reveals that the conversion and propene selectivity are inversely related consistent with the previous results [32]. Furthermore, the selectivity at iso-conversion increases as the phosphorous content in the catalyst increases. For example, at 2.3 % propane conversions the propene selectivities are: 72 % for 3VTi, 81% for 2V1PTi, 82 % for 1V1PTi and 86% for 1V2PTi. Consequently the propene yields at iso-conversion follows the trend: 1V1PTi > 1V2PTi > 2V1PTi > 3VTi. Ciambelli et. al. [32] also observed similar results during the contact time study in the ODH of ethane.

### *iii. Data for Kinetic-Parameter Estimation*

For obtaining the data required for kinetic-parameter estimation, the propane ODH reaction was performed over the modified and unmodified catalysts. Based on the component areas, the component mole fraction are calculated and used to determine the conversion, selectivities, yields and C-balance values. For each catalyst the various yields versus temperature at specific $C_3H_8$:$O_2$ ratios are given in Tables 4.2 to 4.5. The data in each table is organized in smaller sets depending on the reaction temperature. For

example, the top set of data provides the different yields at 613 K for increasing $C_3H_8$:$O_2$ molar ratios. The second set of data provides the different yields at 633 K for increasing $C_3H_8$:$O_2$ molar ratios. Similarly, the third and fourth data sets provide the different yields at 653 and 673 K, respectively.

The data given in Tables 4.2 to 4.6 reveal that the $C_3H_6$, CO and $CO_2$ yields decrease with an increase in $C_3H_8$:$O_2$ molar ratio suggesting that oxidized conditions are beneficial for increasing the yields. Similar conclusions were obtained by Gao et. al. for $V_2O_5/ZrO_2$ catalysts [11]. Furthermore, comparison of the different yields at a particular $C_3H_8$:$O_2$ molar ratio with increasing temperature reveals that all the yields increase suggesting that temperature is also beneficial for increasing the yields. Comparison between the different catalysts is not directly possible since different catalyst amounts have been considered. An appropriate comparison would involve comparison of the yields at equal contact times. Comparison at equal contact times is possible once the kinetic-parameter are estimated.

## *4.3 Kinetic-Parameter Estimation*

Based on the input and output mole fractions the kinetic-parameters for PL-1 and PL-2 models described in section 3.4 are determined by minimizing the objective function. The objective function was the determinant given by Eqn. 3.10. Based on the determinant value obtained after minimization the choice of the model more representative of the reaction data is possible. This is more so since the number of kinetic-parameters used in PL-1 and PL-2 models are the same. The determinant values of the four catalysts are given in Table 4.6 for the two power-law models. Comparison of the determinant values reveals that the values for PL-1 are smaller than or equal to those for PL-2. Consequently,

for comparison purposes the PL-1 model can be used for all the catalysts. The kinetic-parameters along with their units for the PL-2 model are given in the Appendix as Table A5.1.

### *i. Predicted Concentration*

The predicted concentration values of $C_3H_8$, $C_3H_6$, $CO_2$ and CO at the 12 experimental conditions given in Table 4.2 to 4.5 are calculated by using the kinetic-parameters obtained for the four catalysts for the PL-1 model. Since the concentrations of unreacted $C_3H_8$ is large in comparison with $C_3H_6$, CO and $CO_2$, the predicted and actual concentrations are first normalized based on the highest concentration values. The normalized predicted versus actual concentrations are plotted in Fig 4.9 for the PL-1 model. Figure 4.9 reveals that a close correspondence exists between the predicted and actual concentrations and the kinetic-parameters properly represent the steady state reaction data.

### *ii. PL-1 Model*

The pre-exponential factors, $k_{i0}$, activation energies, $E_i$ and component pressure exponents $a_i$ and $b_i$ for the unmodified and phosphorous-modified VTi catalysts using the PL-1 model are calculated at $P_{m(C_3H_8)}$ = 0.2958 atm, $P_{m(O_2)}$ = 0.148 atm and $T_m$ = 643.16 K, and are presented in Table 4.7. The $P_{m(C_3H_6)}$ value, which is different for the four catalysts, is given in the last row of the table. The first column of Table 4.7 contains the 12 kinetic-parameters for the PL-1 model. The second column contains the units of the kinetic-parameters. Finally, the last four columns contain the kinetic-parameter values for the 3VTi, 2V1PTi, 1V1PTi and 1V2PTi catalysts.

Analysis of the values given in Table 4.7 reveals that all the three pre-exponential factors, $k_{i0}$, decrease with increasing phosphorous content. Furthermore, the $k_{20}$ and $k_{30}$ values are similar for each catalyst. The $E_1$ value appears to be constant for the 3VTi, 2V1PTi and 1V1PTi catalysts, whereas the $E_2$ and $E_3$ values appear to increase with phosphorous content for the 3VTi, 2V1PTi and 1V1PTi catalysts. The corresponding $E_1$, $E_2$ and $E_3$ values for 1V2PTi are, however, the smallest. Values of $a_1$ and $b_1$ suggest that reaction $r_1$ (see Fig. 3.3) is first order with respect to propane and half-order with respect to oxygen except for 1V2PTi, where the reaction is zero order with respect to oxygen. The values of $a_2$ and $b_2$ suggest that reaction $r_2$ (see Fig. 3.3) is appears to be half-order with respect to propene and zero order with respect to oxygen. Finally, the $a_3$ values reveal that reaction $r_3$ (see Fig. 3.3) is first order with respect to propene; however, no specific trend is evident for $b_3$.

### *iii. MVK-1 Model*

The MVK-1 model is based on the reaction scheme of the PL-1 model where CO and $CO_2$ are considered to be secondary products. It has eight kinetic-parameters: four pre-exponential factors, $k_{i0}$, and four activation energies, $E_i$. All of the kinetic-parameters are calculated at the mean reaction temperature of 643 K and are given in Table 4.8. This table contains six columns. The first column in Table 4.8 represents the kinetic-parameters, the second column provides the units of these kinetic-parameters, and the third to sixth columns provide the values of these parameters along with the standard error values in parenthesis for the 3VTi, 2V1PTi, 1V1PTi and 1V2PTi catalysts. The standard error values suggest that the kinetic-parameters are determined with a significant degree of accuracy. Based on the kinetic-parameter values for the PL-1 model the

predicted and actual concentrations are compared in Fig.4.9. Similar to the PL-1 model, the MVK-1 model also properly represents the steady state reaction data. By comparing Figs. 4.9 and 4.10 it is not evident, which of the two models represents the steady state reaction data better. It should noted that kinetic-parameters did not converge for the MVK-2 model.

Similar to the PL-1 model the pre-exponential factors, $k_{i0}$, for the MVK-1 model given in Table 4.8 also decrease with an increase in phosphorous content and the $k_{20}$ and $k_{30}$ values are similar for each catalyst. In contrast to the PL-1 model, however, the activation energies values, $E_i$, appear to be similar for the 3VTi, 2V1PTi and 1V1PTi catalysts. For the 1V2PTi catalyst, the activation energy values are significantly lower than the other catalysts.

Analysis of the kinetic–parameters obtained for the four catalysts using the PL-1 and MVK-1 models suggest that with an increase in phosphorous content the pre-exponential factors gradually decrease suggesting that the sites involved with these reactions are progressively poisoned. The decrease in sites is consistent with decreasing trend of H/V ratios with an increase in phosphorous content. To observe the decrease in the $k_{i0}$ values, the pre-exponential factors normalized with the pre-exponential factor for 3VTi, $(k_{i0})_{normalized}$, is plotted for the four catalysts and the two models in Fig. 4.11. Fig. 4.11 reveals that the $k_{i0}$ values decreases with an increase in phosphorous content, however, the relative decrease is different. For example, the $k_{20}$ and $k_{30}$ values decrease more than sharply in comparison to the decrease in $k_{10}$ values. The $k_{40}$ value of the MVK-1 model decreases the most amongst all the pre-exponential factors. Thus, the relative poisoning of the sites responsible for the $r_1$, $r_2$, $r_3$ and $r_4$ reactions are different.

The pre-exponential factor usually corresponds to the number of active sites or the activity per site. Consequently, the number of active sites or the activity per site or both decrease with an increase in phosphorous content. Comparison of the three activation energy values for the 3VTi, 2V1PTi and 1V1PTi catalysts given by the mechanistic MVK-1 model suggest that the catalytic cycles involved in reactions $r_1$ to $r_4$ are similar. The 1V2PTi sample shows different $E_i$ values suggesting that a different species is involved. This is consistent with the TPR profile since a second reduction peak corresponding to a different reducible site is present. The EPR spectra does reveal that a different paramagnetic $V^{+4}$ species is present. However, no information regarding the $V^{+5}$ species is given. Thus, the number or activity per active site progressively decreases, however, the activation energies involved in propane conversion to propene and propene conversion to $CO_x$ are independent of phosphorous content till a V: P ratio of 1:1. For higher phosphorous content a new reducible species is formed that gives rise to different activation energies during propane ODH.

The degree of reduction, β, given by in the MVK-1 model is plotted versus propane conversion in Fig. 4.12 for the unmodified and phosphorous-modified VTi catalysts. It is observed that the degree of reduction increases with an increase in propane conversion. At iso-conversion the degree of reduction is the same for all the catalysts at low conversion values (< 5 %). At high conversions, however the degree of reduction follows the trend: 3VTi > 2V1PTi > 1V1PTi > 1V2PTi. Thus, at low conversions the fraction of oxidized and reduced sites are the same for the unmodified and phosphorous-modified VTi catalysts, but at high conversions the fraction of reduced sites are the most for the 3VTi.

The kinetic-parameters can also be used to obtain the optimum reactor operating conditions and for catalyst design. The rate constants $k_i$, depend on the values of $k_{i0}$, $E_i$ and temperature of the reaction. Furthermore, the rate constant $k_1$, is related to the desirable propane ODH reaction and the rate constants $k_2$ and $k_3$ are related to the undesirable propene degradation reaction. For a consecutive reaction mechanism as in the PL-1 and MVK-1 models chosen here, the propene yield depends on the contact time and $(k_2+k_3)/k_1$ value [62]. With a change in contact time the propene yield increases and then decreases. The yield at optimum contact time is a function of the $(k_2+k_3)/k_1$ ratio. For a particular catalyst the $(k_2+k_3)/k_1$ ratio can be changed by changing the temperature. For example, in the present study the $(k_2+k_3)/k_1$ ratio decreases with an increase in temperature. Consequently, the contact time where the propene yield is optimum is also a function of temperature. This is clearly shown in Fig. 4.13 where the predicted propene yield for the 3VTi catalyst is plotted versus the contact time for different $(k_2+k_3)/k_1$ values corresponding to different temperatures. The $C_3H_8$:$O_2$ ratio chosen is 2:1. It is observed that for the PL-1 model an optimum contact time is observed, whereas for the MVK-1 model oxygen is depleted before the propene yield reaches a maximum. Comparing the propene yield at a particular contact time for different $(k_2+k_3)/k_1$ values suggests that the propene yield increases as the $(k_2+k_3)/k_1$ decreases or the reaction temperature increases. The increase in propene yield with temperature is consistent with the data given in Tables 4.2 to 4.5. Additionally, for the PL-1 model the contact time where the propane yield is maximum also increases with an increase in $(k_2+k_3)/k_1$ value. Similar trends are observed for first-order consecutive reactions [62]. Thus, the reaction can be operated at the proper contact time for achieving maximum propene yield at a

propene yields and selectivities and the similar ESR spectra and TPR profile of the two samples suggest that the MVK-1 model is more appropriate to represent the data.

Thus, with proper characterization and kinetic-parameter estimation it is possible to obtain the structure-reactivity relationships showing the effect of phosphorous modification over the vanadia-titania catalyst. The decrease in conversion with phosphorous addition to the vanadia-titania catalyst is related to the decrease in the pre-exponential factor, $k_{i0}$, suggesting that the number of active sites and/or activity per site are/is decreasing. However, the relative decrease in the pre-exponential factors, $k_{i0}$'s, and consequently the number of active sites and/or activity per site is different with phosphorous modification. As a result the $(k_2+k_3)/k_1$ value decreases with an increase in phosphorous content. Consequently, the propene yield or propene selectivity at iso-conversion increases with an increase in phosphorous content.

**Table 4.1: Surface area, $T_{max}$ and H/V ratio of the catalysts**

| Sl. No. | Nomenclature | Surface area ($m^2/g$) | $T_{max}$ (K) | H/V Ratio |
|---|---|---|---|---|
| 1 | $TiO_2$ | 43 | - | - |
| 2 | 3VTi | 43 | 718 | 2.0 |
| 3 | 2V1PTi | 42 | 751 | 1.6 |
| 4 | 1V1PTi | 41 | 751 | 1.4 |
| 5 | 1V2PTi | 41 | 778, 862 | 1.3 |
| 6 | 1.2PTi | 47 | 820 | - |
| 7 | 4.6PTi | 41 | - | - |

**Table 4.2: Catalytic results of propane ODH for 3VTi catalyst.**

**Weight of the catalyst = 0.03 g; Total flow rate =75ml/min**

| Reaction Temperature (K) | $C_3H_8/O_2$ ratio | Yield (%) | | | C-balance ($C_{out}/C_{in}$) |
|---|---|---|---|---|---|
| | | $C_3H_6$ | $CO_2$ | CO | |
| 613 | 1:1 | 0.60 | 0.03 | 0.07 | 0.998 |
| | 2:1 | 0.55 | 0.02 | 0.05 | 0.998 |
| | 3:1 | 0.51 | 0.02 | 0.04 | 0.999 |
| 633 | 1:1 | 0.97 | 0.06 | 0.12 | 0.988 |
| | 2:1 | 0.86 | 0.06 | 0.10 | 0.993 |
| | 3:1 | 0.79 | 0.05 | 0.08 | 0.996 |
| 653 | 1:1 | 1.42 | 0.12 | 0.23 | 0.994 |
| | 2:1 | 1.31 | 0.10 | 0.19 | 0.999 |
| | 3:1 | 1.20 | 0.09 | 0.16 | 0.966 |
| 673 | 1:1 | 1.99 | 0.21 | 0.41 | 0.917 |
| | 2:1 | 1.92 | 0.22 | 0.38 | 0.979 |
| | 3:1 | 1.75 | 0.19 | 0.33 | 0.951 |

**Table 4.3: Catalytic results of propane ODH for 2V1PTi catalyst.**

**Weight of the catalyst = 0.04 g; Total flow rate = 75ml/min**

| Reaction Temperature (K) | $C_3H_8/O_2$ ratio | Yield (%) | | | C-balance ($C_{out}/C_{in}$) |
|---|---|---|---|---|---|
| | | $C_3H_6$ | $CO_2$ | CO | |
| 613 | 1:1 | 0.60 | 0.02 | 0.04 | 1 |
| | 2:1 | 0.50 | 0.01 | 0.03 | 0.996 |
| | 3:1 | 0.45 | 0.01 | 0.02 | 1.002 |
| 633 | 1:1 | 0.94 | 0.05 | 0.08 | 1.003 |
| | 2:1 | 0.88 | 0.03 | 0.06 | 0.999 |
| | 3:1 | 0.73 | 0.03 | 0.05 | 0.975 |
| 653 | 1:1 | 1.37 | 0.08 | 0.14 | 1.008 |
| | 2:1 | 1.27 | 0.07 | 0.11 | 1.001 |
| | 3:1 | 1.12 | 0.05 | 0.09 | 0.972 |
| 673 | 1:1 | 2.19 | 0.18 | 0.31 | 1.018 |
| | 2:1 | 1.97 | 0.16 | 0.25 | 0.999 |
| | 3:1 | 1.83 | 0.13 | 0.21 | 0.949 |

**Table 4.4: Catalytic results of propane ODH for 1V1PTi catalyst.**

**Weight of the catalyst = 0.10 g; Total flow rate =75ml/min**

| Reaction Temperature (K) | $C_3H_8/O_2$ ratio | Yield (%) | | | C-balance ($C_{out}/C_{in}$) |
|---|---|---|---|---|---|
| | | $C_3H_6$ | $CO_2$ | CO | |
| 613 | 1:1 | 0.70 | 0.03 | 0.05 | 0.996 |
| | 2:1 | 0.60 | 0.02 | 0.03 | 0.999 |
| | 3:1 | 0.46 | 0.01 | 0.02 | 0.999 |
| 633 | 1:1 | 1.03 | 0.06 | 0.10 | 0.998 |
| | 2:1 | 0.94 | 0.04 | 0.07 | 0.986 |
| | 3:1 | 0.77 | 0.03 | 0.04 | 0.994 |
| 653 | 1:1 | 1.46 | 0.10 | 0.19 | 0.989 |
| | 2:1 | 1.36 | 0.08 | 0.13 | 0.964 |
| | 3:1 | 1.21 | 0.06 | 0.09 | 0.997 |
| 673 | 1:1 | 2.27 | 0.19 | 0.34 | 0.992 |
| | 2:1 | 2.15 | 0.18 | 0.30 | 0.943 |
| | 3:1 | 1.97 | 0.14 | 0.23 | 0.988 |

**Table 4.5: Catalytic results of propane ODH for 1V2PTi catalyst.**

**Weight of the catalyst = 0.20 g; Total flow rate =75ml/min**

| Reaction Temperature (K) | $C_3H_8/O_2$ ratio | Yield (%) | | | C-balance ($C_{out}/C_{in}$) |
|---|---|---|---|---|---|
| | | $C_3H_6$ | $CO_2$ | CO | |
| 613 | 1:1 | 0.52 | 0.01 | 0.02 | 0.992 |
| | 2:1 | 0.43 | 0.01 | 0.02 | 0.998 |
| | 3:1 | 0.47 | 0.01 | 0.01 | 0.982 |
| 633 | 1:1 | 0.82 | 0.02 | 0.04 | 0.975 |
| | 2:1 | 0.66 | 0.01 | 0.02 | 0.992 |
| | 3:1 | 0.74 | 0.01 | 0.03 | 0.989 |
| 653 | 1:1 | 1.15 | 0.03 | 0.06 | 0.958 |
| | 2:1 | 1.02 | 0.02 | 0.04 | 0.981 |
| | 3:1 | 1.07 | 0.02 | 0.04 | 0.985 |
| 673 | 1:1 | 1.72 | 0.05 | 0.11 | 0.957 |
| | 2:1 | 1.49 | 0.05 | 0.07 | 0.982 |
| | 3:1 | 1.51 | 0.04 | 0.07 | 0.983 |

**Table 4.6: Comparison of determinant values of PL-1 and PL-2 model**

| Catalyst | Determinant Value for PL-1 Model | Determinant Value for PL-2 Model |
|---|---|---|
| **3VTi** | 2.41E-30 | 4.00E-30 |
| **2V1PTi** | 6.25E-30 | 6.88E-30 |
| **1V1PTi** | 2.48E-29 | 2.48E-29 |
| **1V2PTi** | 2.16E-31 | 2.16E-31 |

**Table 4.7: Kinetic parameters for the four catalysts following PL-1 Model**

| Parameter | Units | Kinetic- Parameter values for the Catalyst | | | |
|---|---|---|---|---|---|
| | | 3VTi | 2V1PTi | 1V1PTi | 1V2PTi |
| $k_{10}$ | $ml\ STP\ min^{-1}\ (g\ cat)^{-1}\ atm^{-(ai+bi)}$ | 9.51 | 6.51 | 2.80 | 0.97 |
| $k_{20}$ | | 1.04 | 0.44 | 0.17 | 0.04 |
| $k_{30}$ | | 0.99 | 0.50 | 0.18 | 0.04 |
| $E_1$ | $kJ\ mol^{-1}$ | 80 | 85 | 83 | 69 |
| $E_2$ | | 64 | 80 | 95 | 55 |
| $E_3$ | | 52 | 58 | 79 | 37 |
| $a_1$ | *Dimensionless* | 1 | 1 | 1 | 1 |
| $b_1$ | | 0.49 | 0.68 | 0.65 | 0 |
| $a_2$ | | 0.82 | 0.70 | 0.52 | 0.62 |
| $b_2$ | | 0 | 0 | 0 | 0 |
| $a_3$ | | 1 | 1 | 0.72 | 1 |
| $b_3$ | | 0 | 0.55 | 0.24 | 0.93 |
| $P_{m(C_3H_6)}$ | *atm* | 0.0033 | 0.0033 | 0.0035 | 0.0028 |

*Calculated at $P_{m(C_3H_8)}$ = 0.2958 atm, $P_{m(O_2)}$ = 0.148 atm, $T_m$ = 643.16 K

**Table 4.8: Kinetic parameters for the four catalysts following MVK-1 model**

| Parameter | Units | Kinetic- Parameter values for the Catalyst | | | |
|---|---|---|---|---|---|
| | | **3VTi (S.E.)** | **2V1PTi (S.E.)** | **1V1PTi (S.E.)** | **1V2PTi (S.E.)** |
| $k_{10}$ | ml STP $min^{-1}$ $(g\ cat)^{-1}$ $atm^{-1}$ | 34 (0.28) | 29 (0.30) | 14 (0.22) | 4 (0.18) |
| $k_{20}$ | | 357 (3) | 204 (21) | 92 (2) | 18 (1) |
| $k_{30}$ | | 328 (3) | 196 (2) | 84 (1) | 17 (1) |
| $k_{40}$ | | 874 (61) | 150 (5) | 52 (2) | 28 (4) |
| $E_1$ | kJ $mol^{-1}$ | 81 (1) | 79 (1) | 70 (1) | 69 (2) |
| $E_2$ | | 51 (1) | 51 (1) | 44 (2) | 30 (3) |
| $E_3$ | | 45 (1) | 52 (1) | 44 (1) | 33 (3) |
| $E_4$ | | 154 (5) | 123 (3) | 137 (3) | 83 (9) |

- $T_m$ = 643.16 K
- S.E. = Standard Error

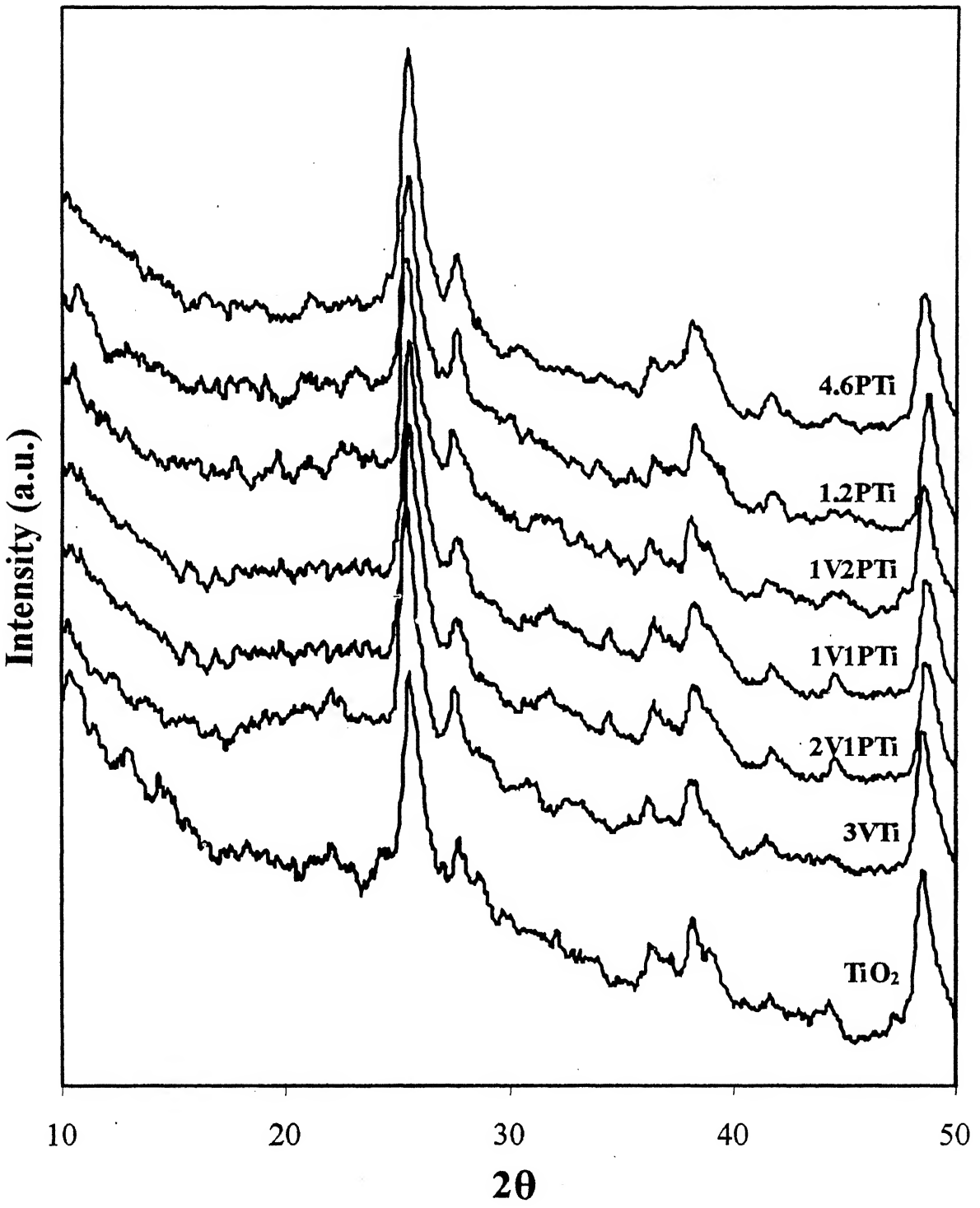


**Figure 4.1: X-ray diffractograms of the $TiO_2$ and titania-supported samples**

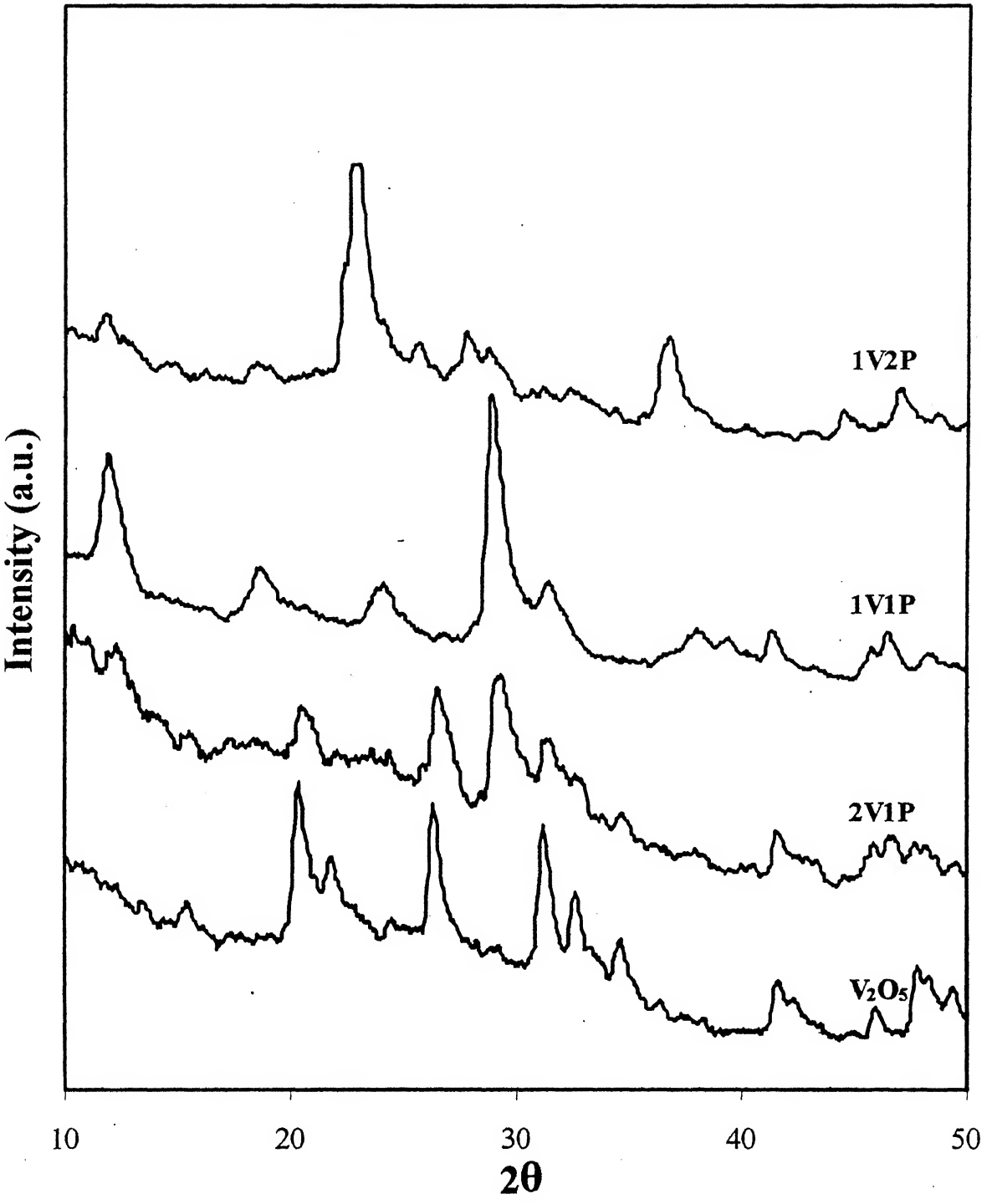


**Figure 4.2: X-ray Diffractograms of unsupported $V_2O_5$ and VPO samples**

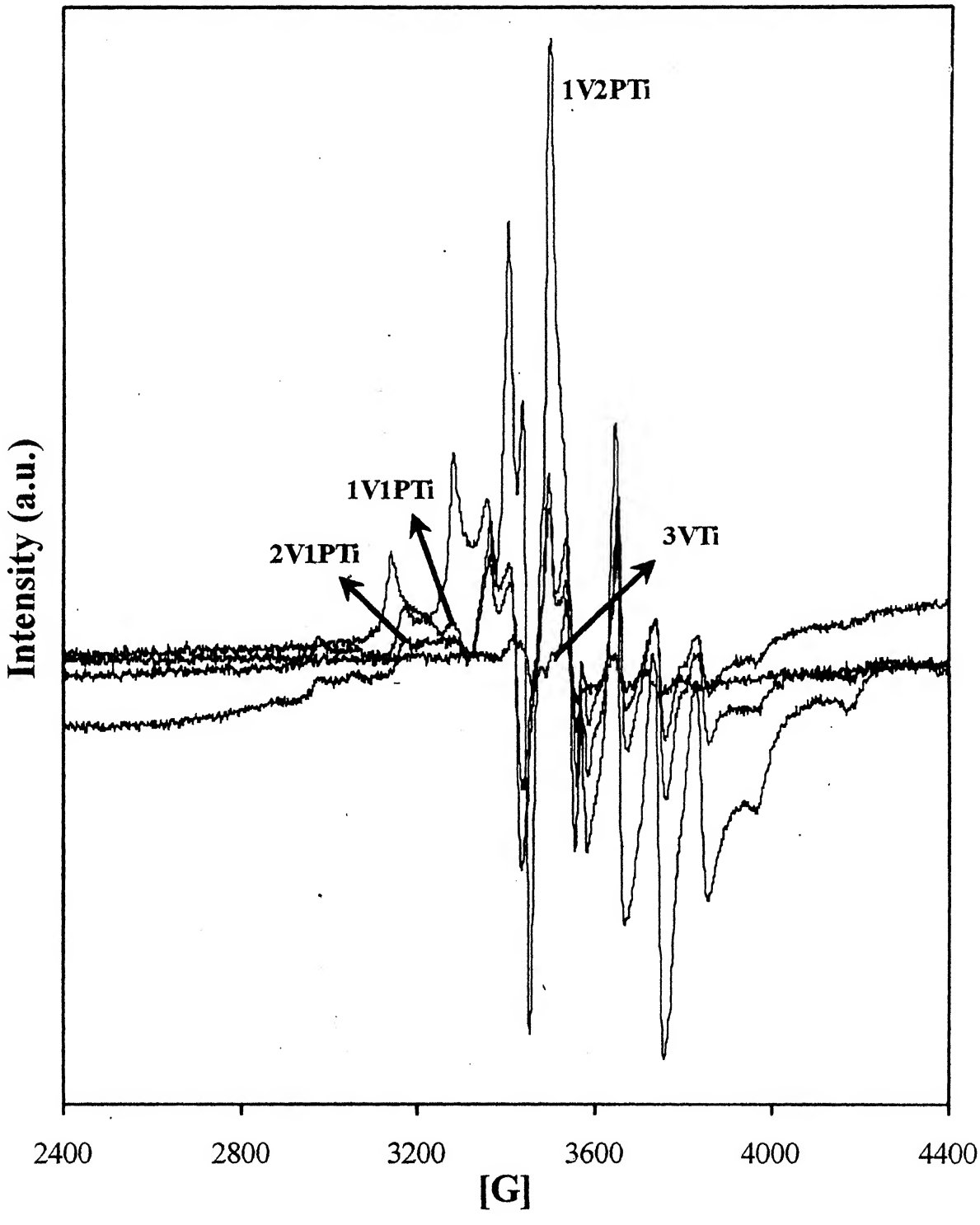


**Figure 4.3: EPR spectra of VTi and phosphorous-modified VTi sample**

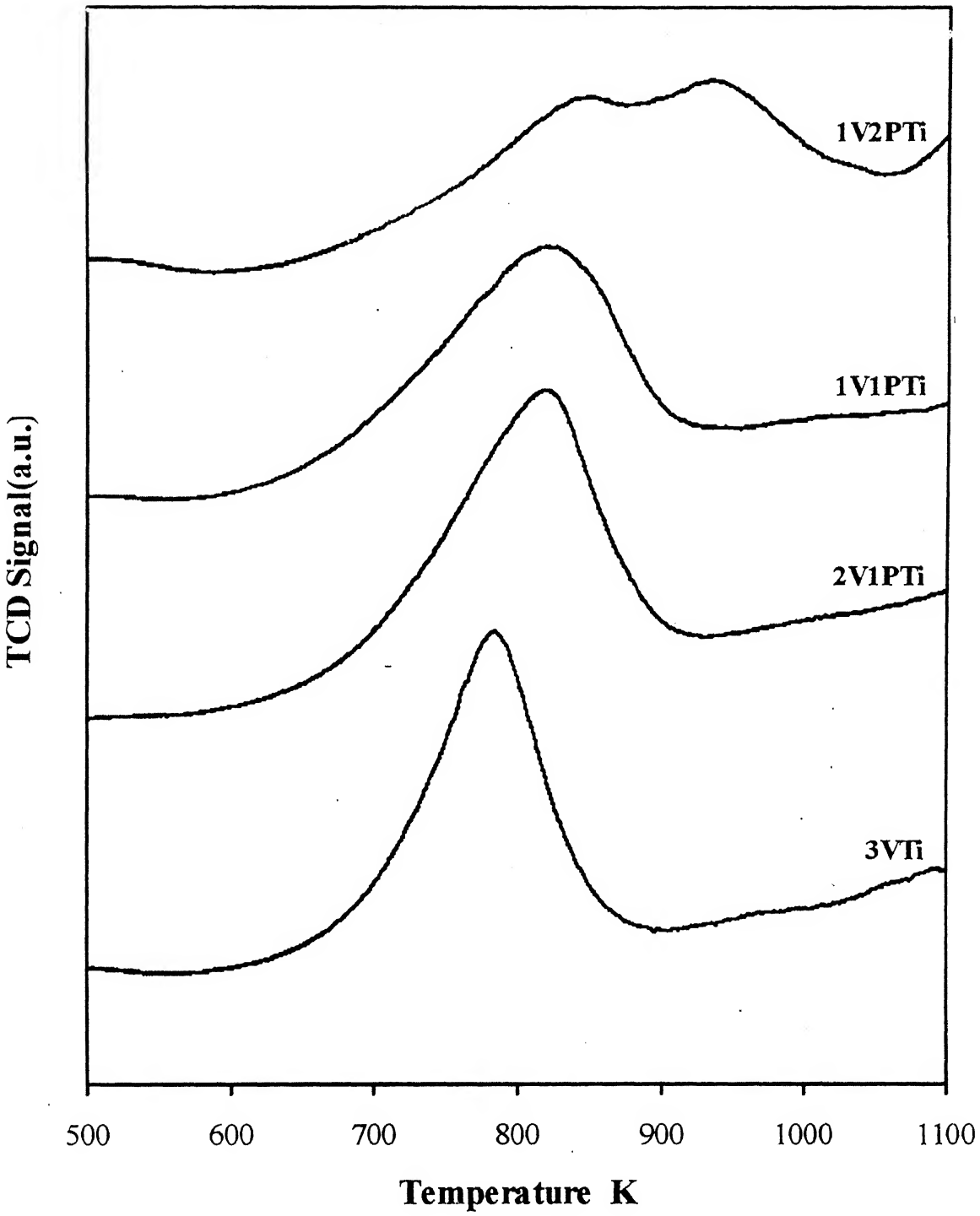


**Figure 4.4: TPR profiles for VTi and phosphorous-modified VTi samples**

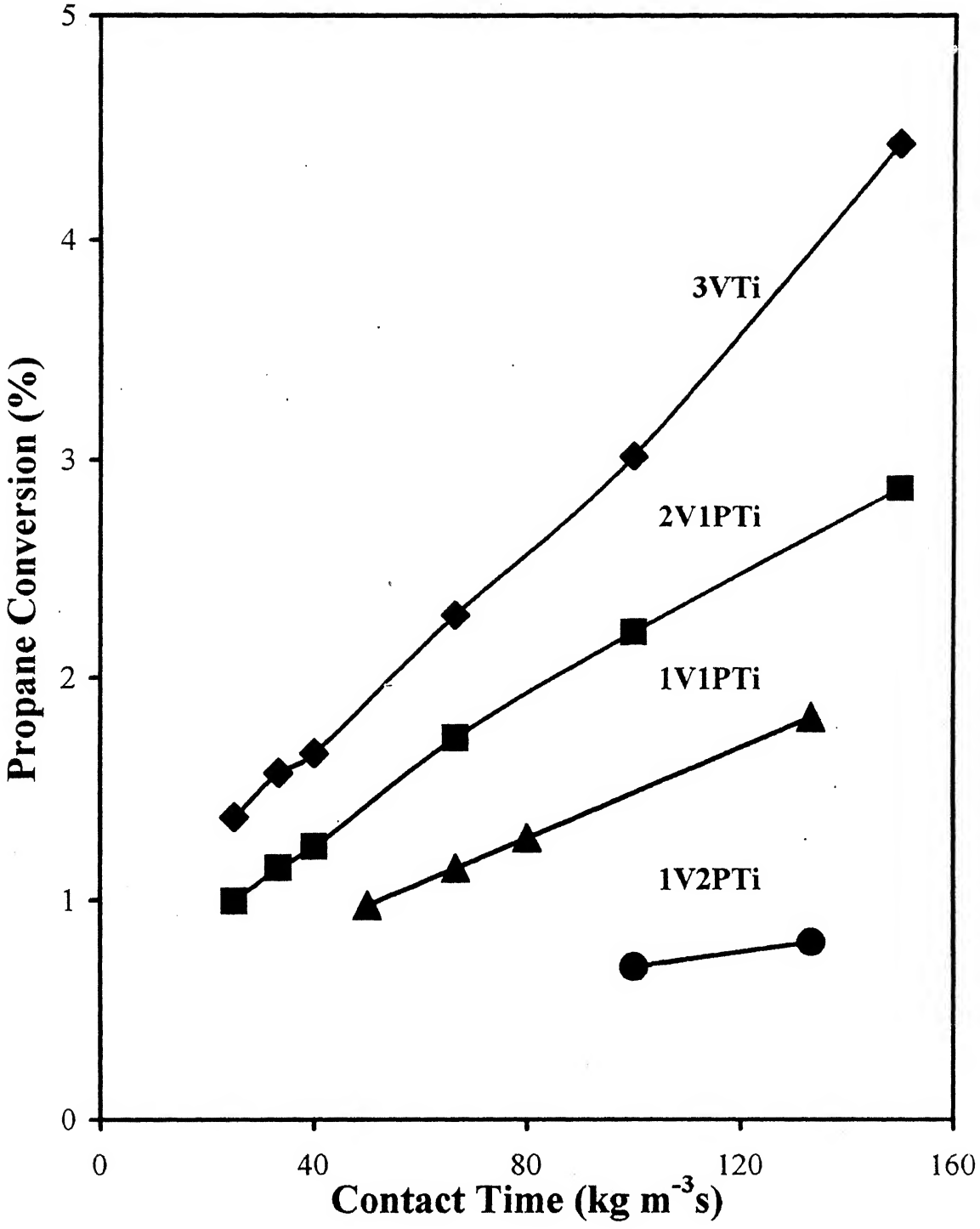


**Figure 4.5: Contact time study: conversion versus contact time for VTi and phosphorous-modified VTi samples. Temperature = 643 K; $C_3H_6$:$O_2$ = 2:1**

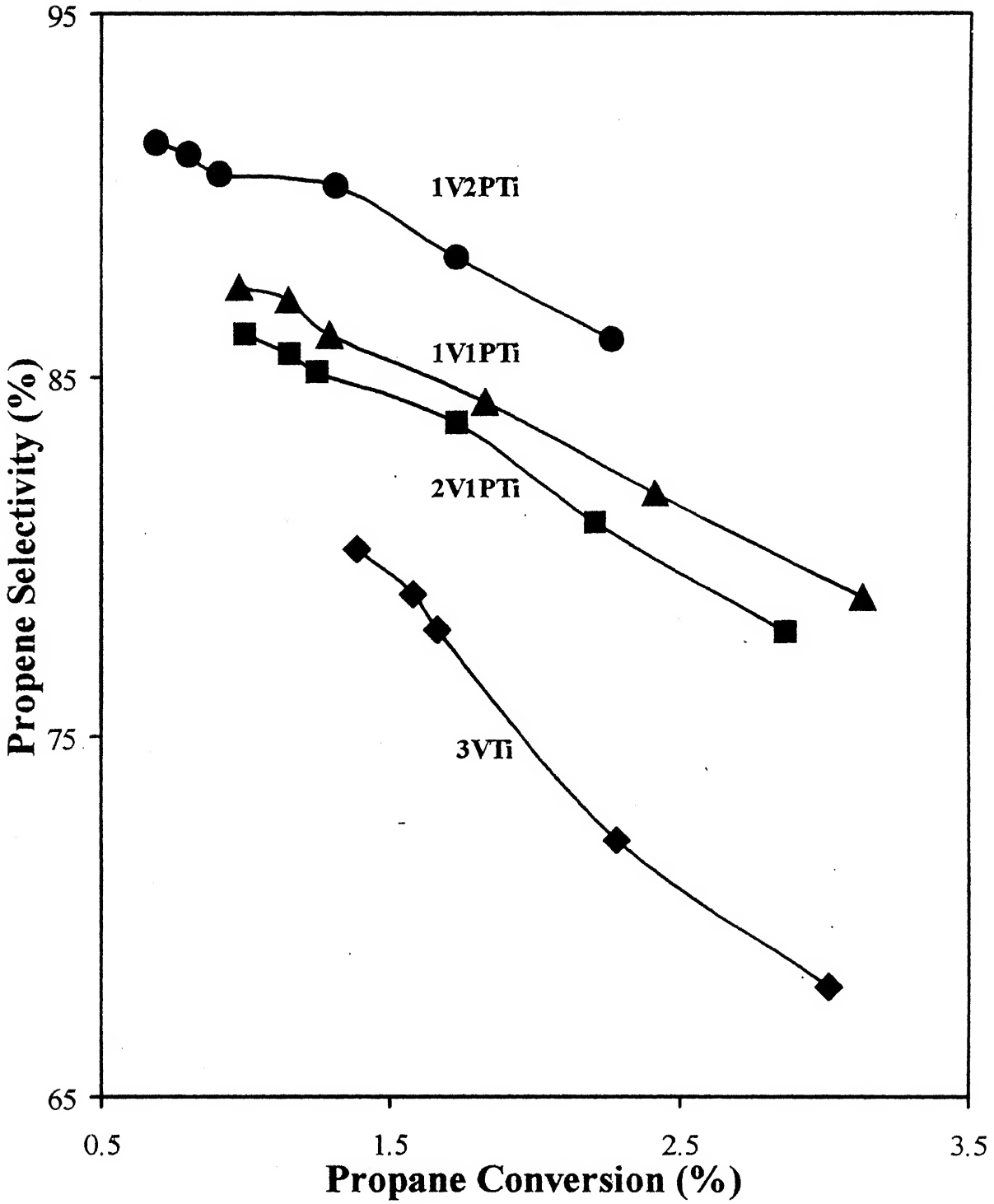


**Figure 4.6: Contact time study: propene selectivity versus propane conversion for VTi and phosphorous-modified VTi samples. Temperature = 643 K; $C_3H_6$:$O_2$ = 2:1**

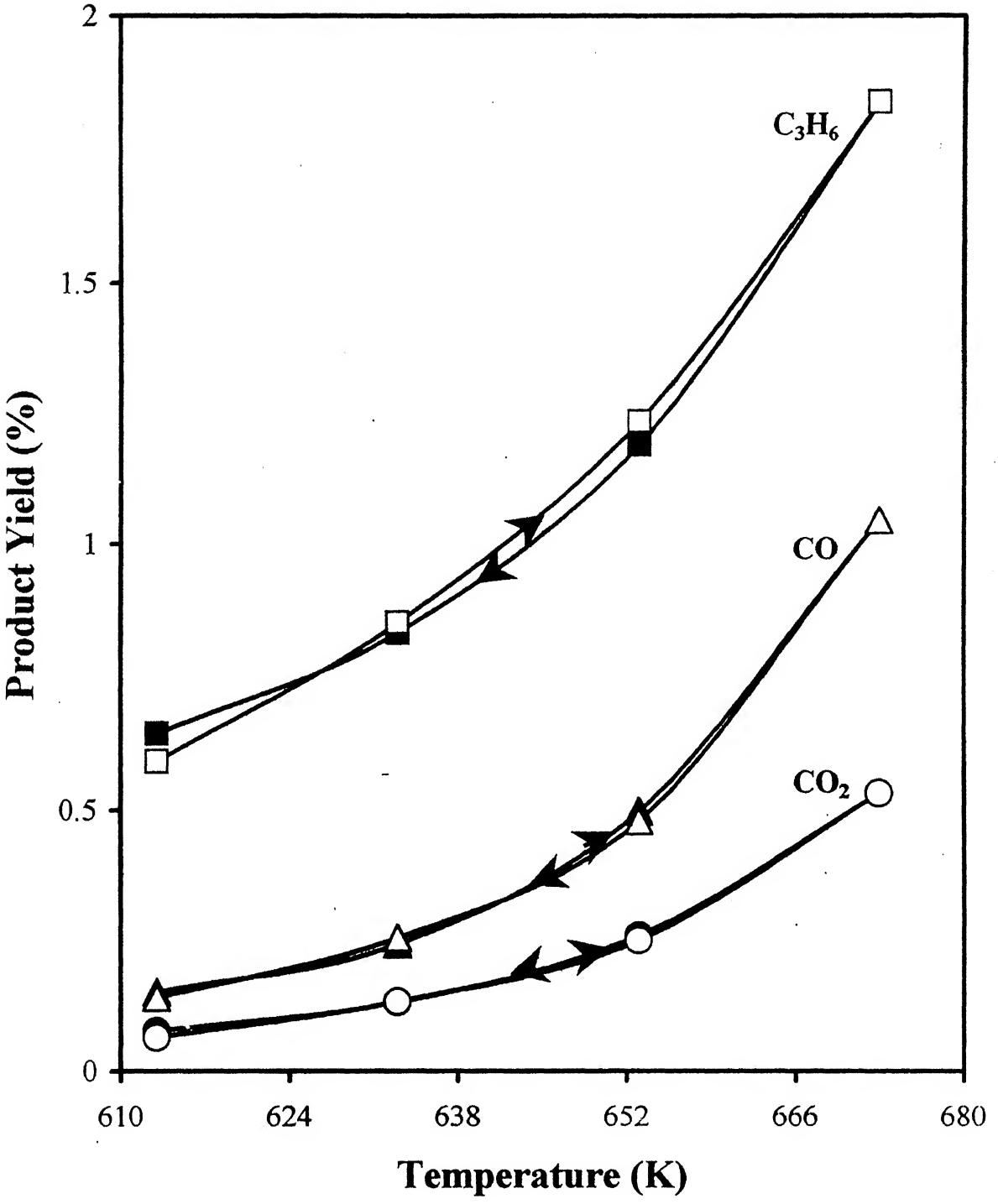


**Figure 4.7: Product yield versus temperature for 3VTi sample showing the reproducibility of propane ODH. Total flow rate = 75 ml/min; $C_3H_6$:$O_2$ = 1:1; wt. of the catalyst = 0.05 g**

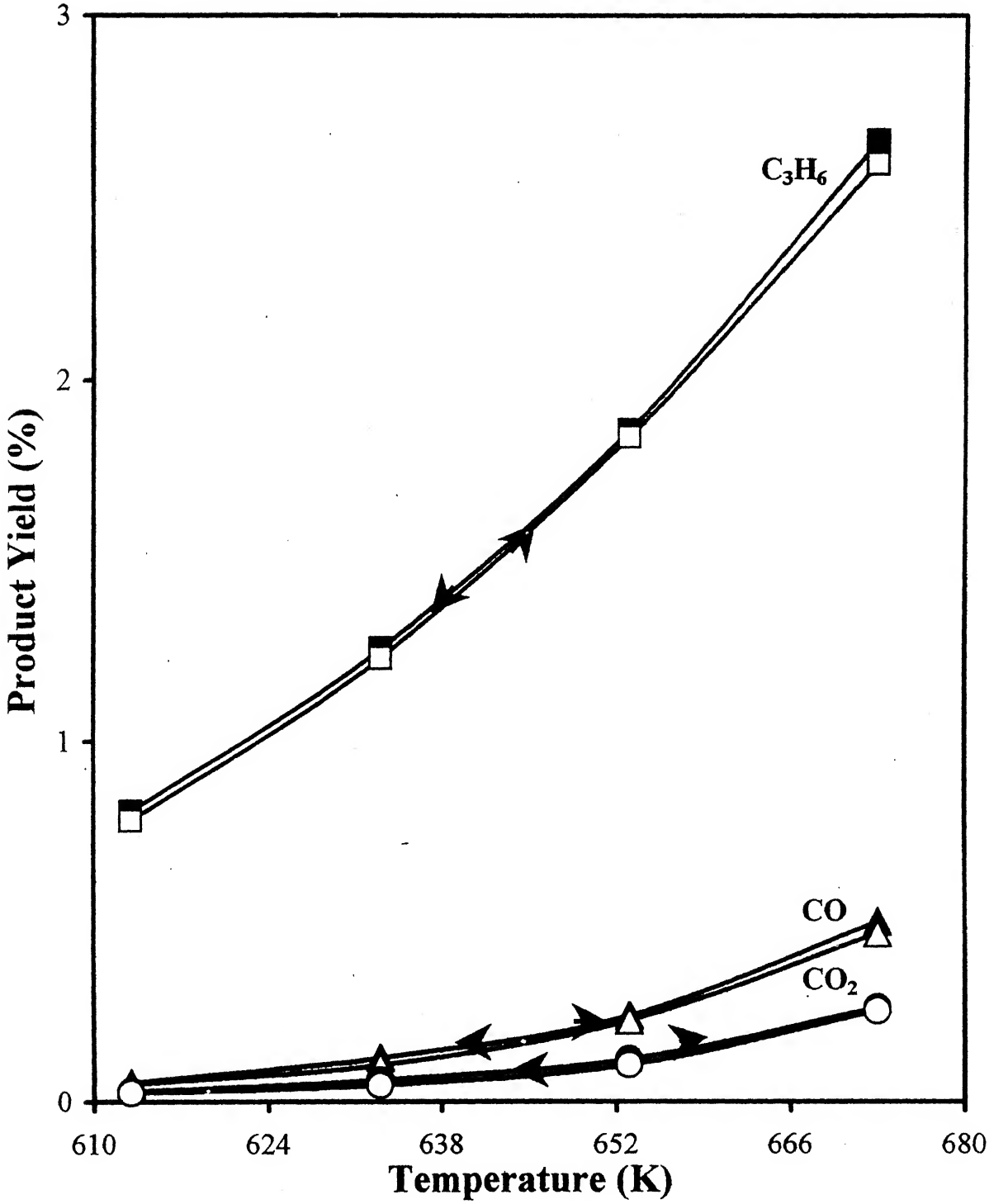


**Figure 4.8: Product yield versus temperature for 1V1PTi sample showing the reproducibility of propane ODH. Total flow rate = 75 ml/min; $C_3H_6$:$O_2$ = 1:1; wt. of the catalyst = 0.10 g**

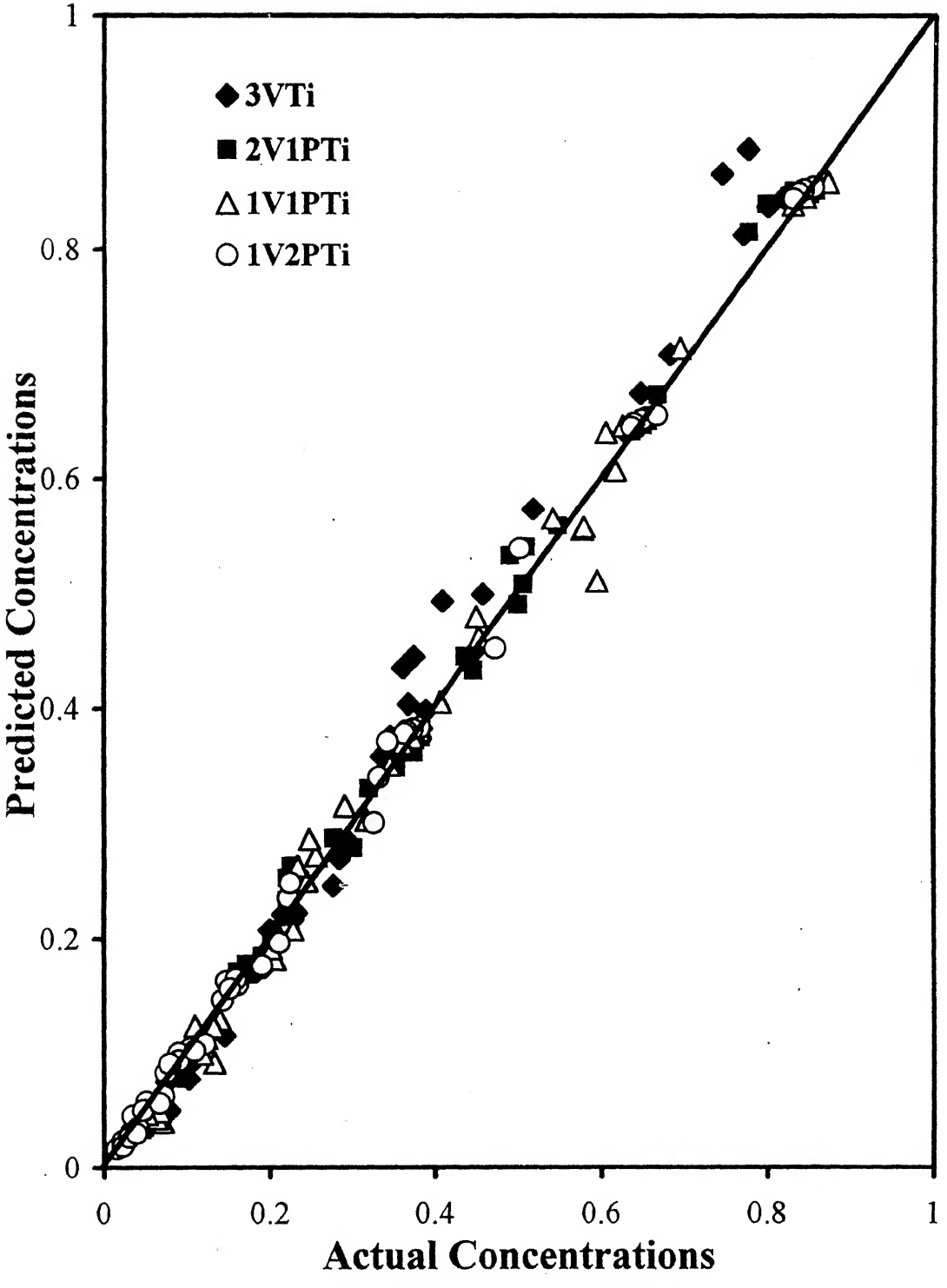


**Figure 4.10: Normalized predicted concentration versus normalized actual concentration for MVK-1 model for VTi and phosphorous-modified VTi samples**

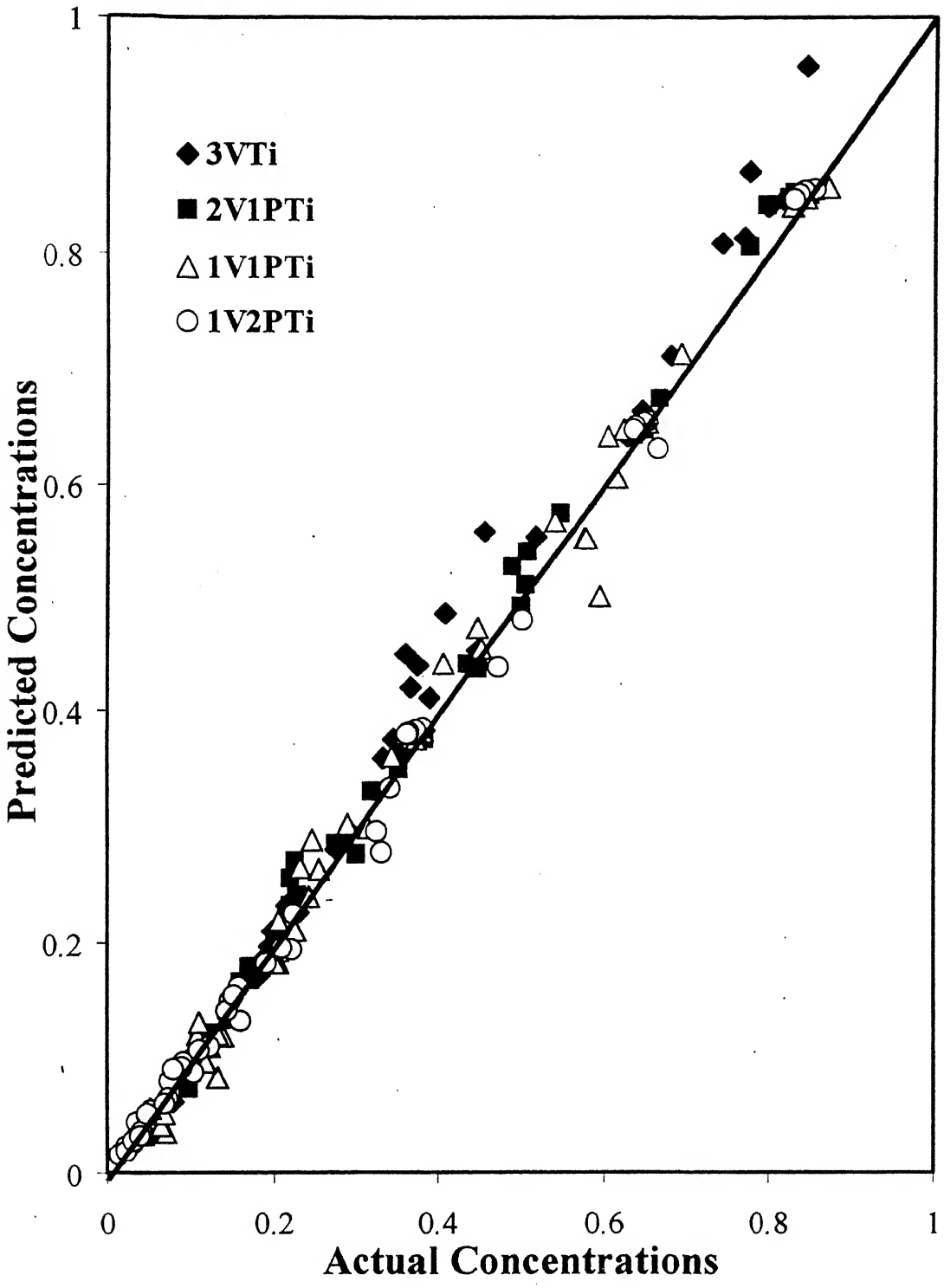


**Figure 4.9: Normalized predicted concentration versus normalized actual concentration for PL-1 model for VTi and phosphorous-modified VTi samples**

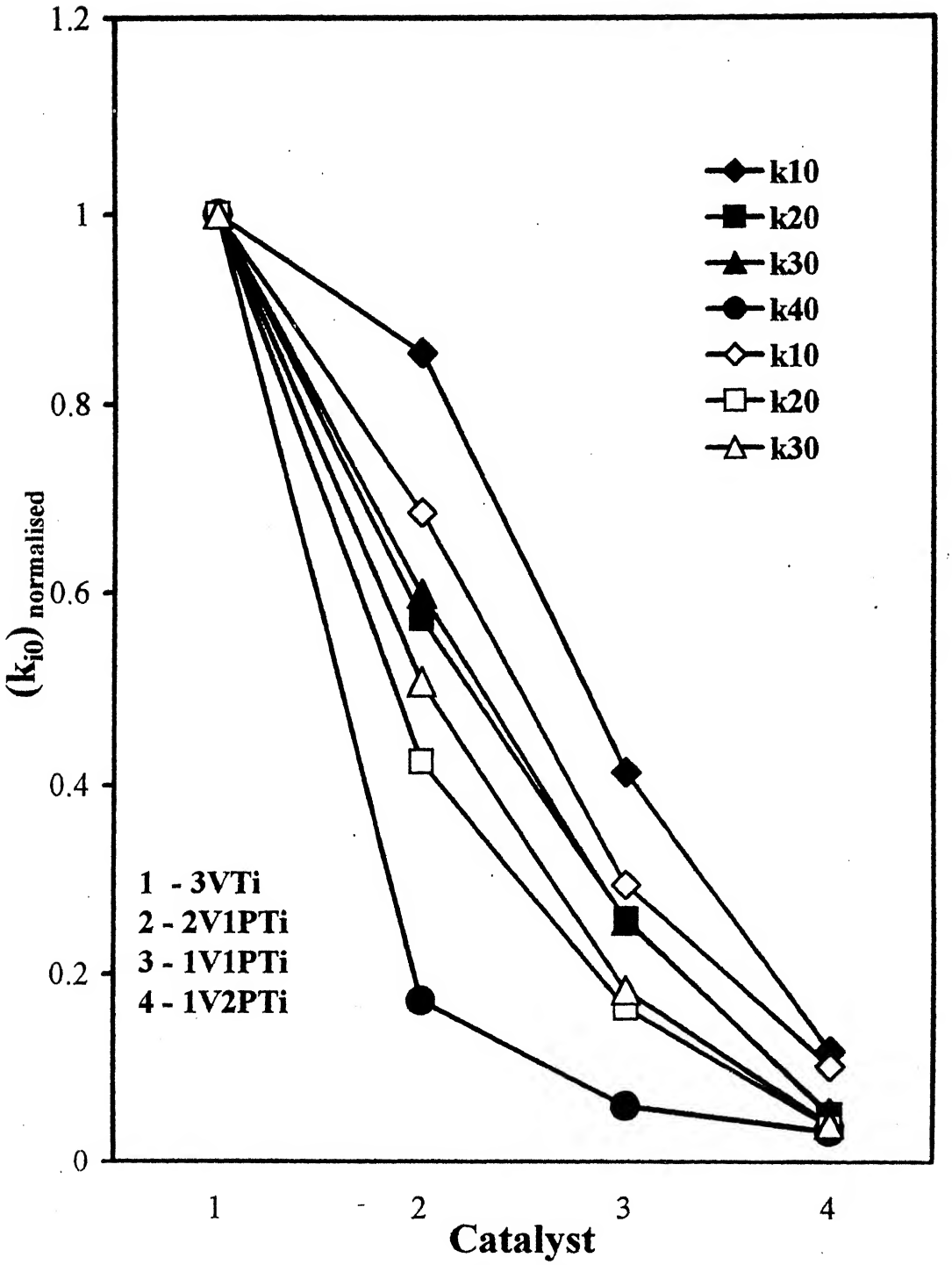


**Figure 4.11: Normalized pre exponential factor for different catalysts using MVK-1 (solid symbols) and PL-1 model (open symbols)**

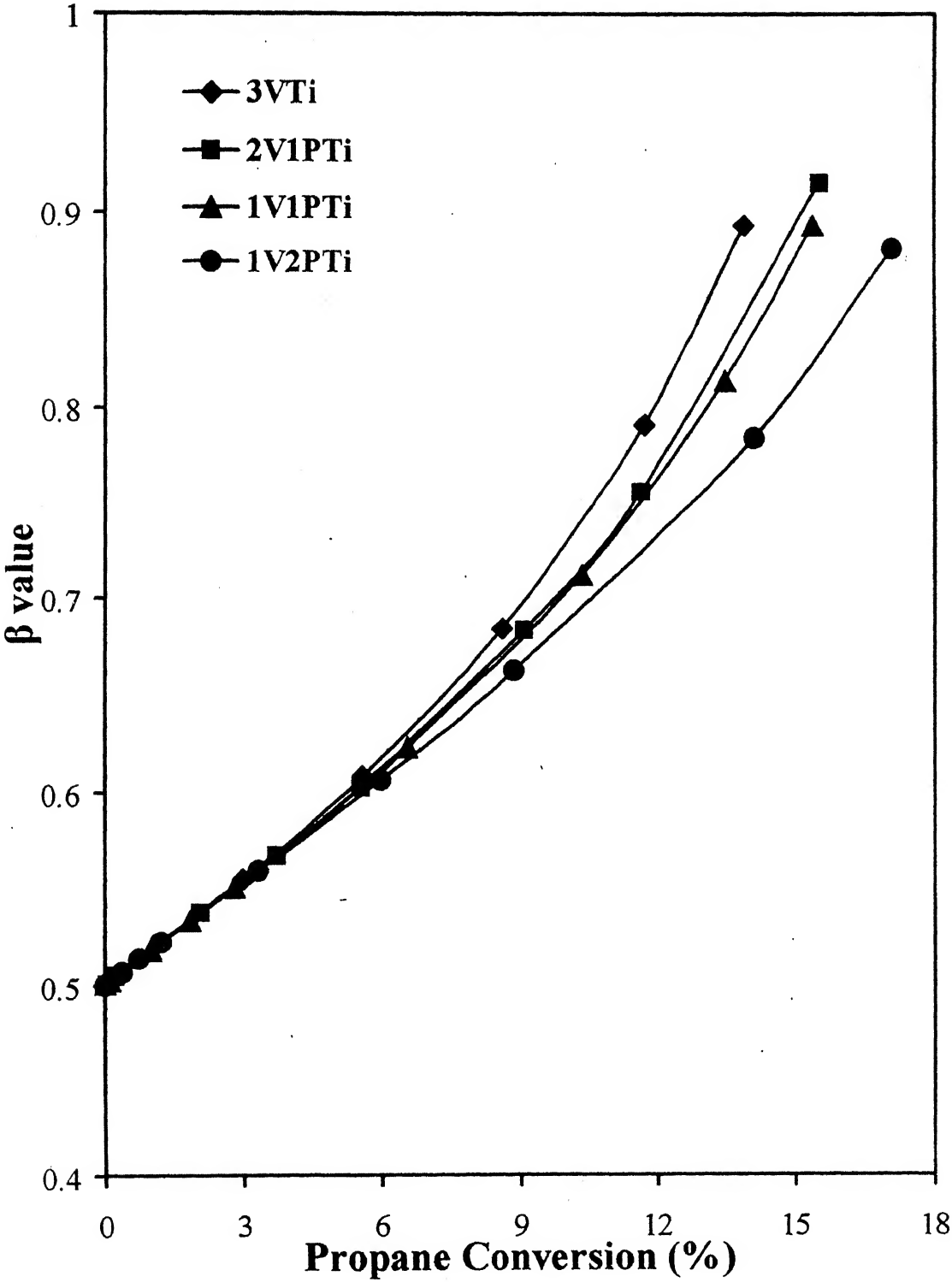


**Figure 4.12: Predicted β value versus propane conversion for VTi and phosphorous-modified VTi samples for MVK-1 model; Temperature = 643 K; $C_3H_6$:$O_2$ = 2:1; wt. of the catalysts = 1.00 g**

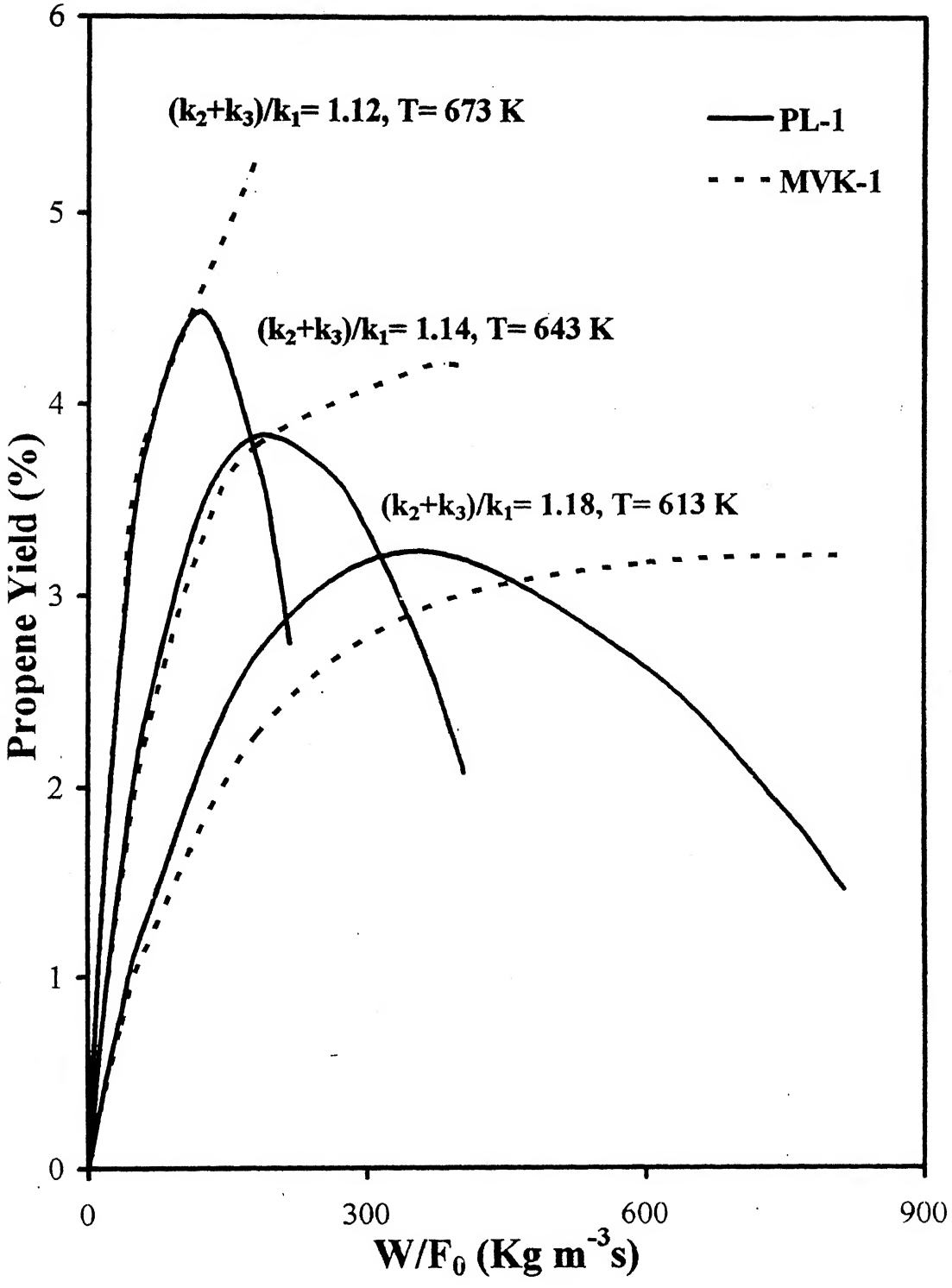


**Figure 4.13: Predicted propene yield versus contact time for 3VTi catalyst wt. of the catalyst = 0.03g; $C_3H_6$:$O_2$ = 2:1**

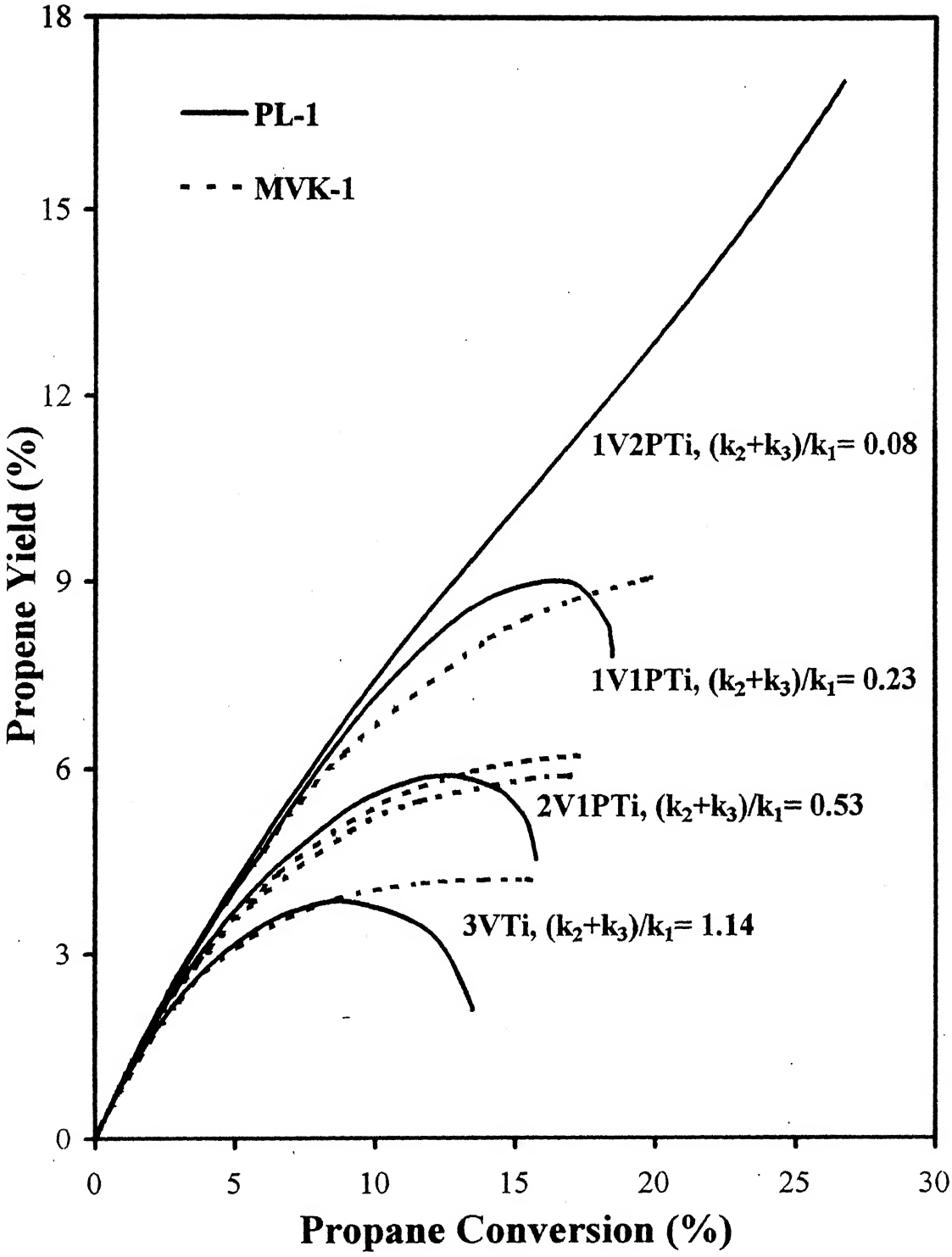


**Figure 4.14: Predicted propene yield versus propane conversion for VTi and phosphorous-modified VTi samples; Temperature = 643 K; $C_3H_6$:$O_2$ = 2:1; wt. of the catalysts = 1.00 g**

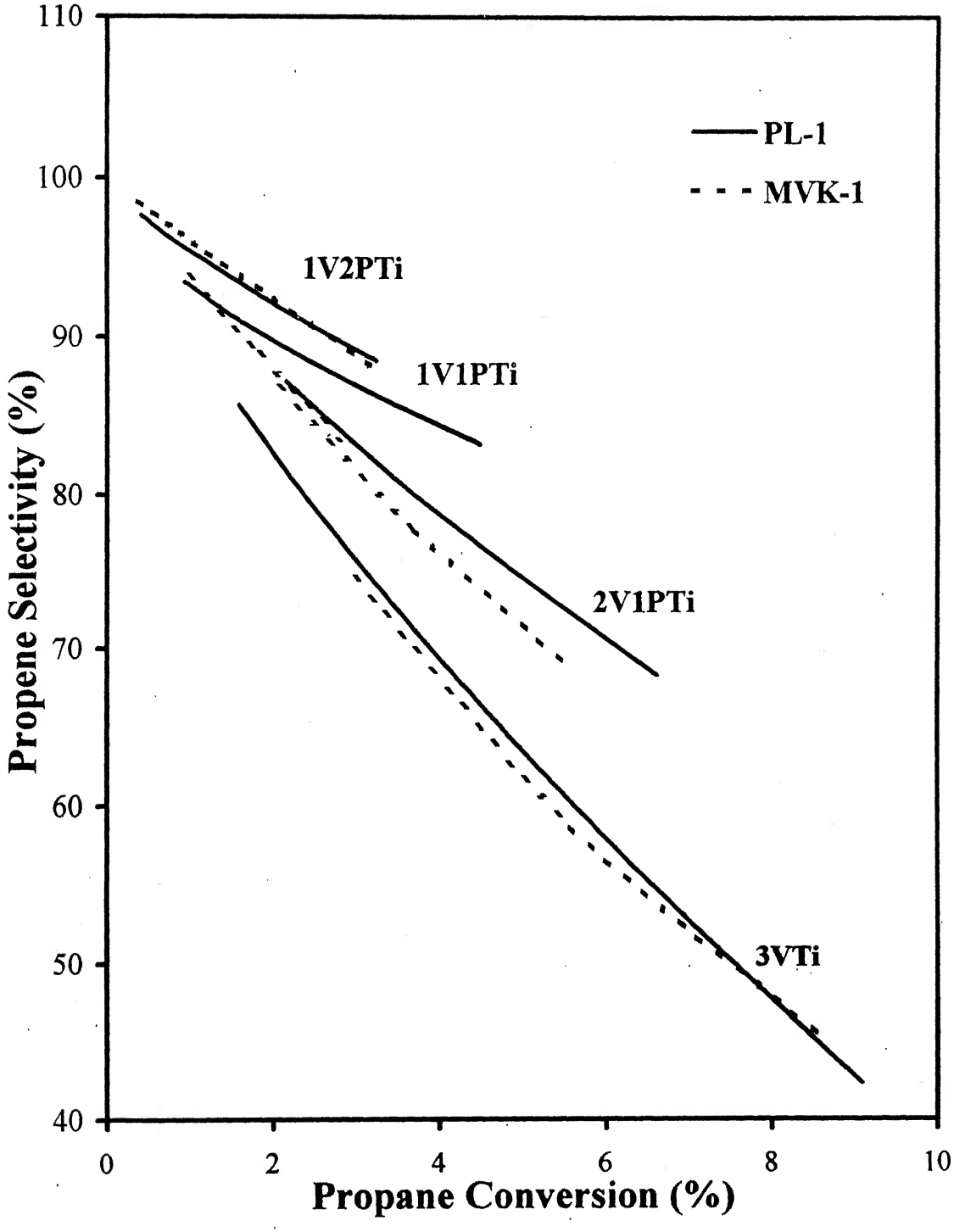


**Figure 4.15: Predicted propene selectivity versus propane conversion for VTi and phosphorous-modified VTi samples; Temperature = 643 K; $C_3H_6$:$O_2$ = 2:1; wt. of the catalysts = 1.00 g**

# Chapter: 5

## *CONCLUSIONS AND RECOMMENDATIONS*

### *5.1 Conclusions*

The objective of present study is carried out to understand the structure-reactivity relationship for titania ($TiO_2$) supported vanadium(V)-phosphorous(P)-oxide(O) catalysts and the ODH of propane. To achieve this objective several VPO/$TiO_2$ catalysts with varying **V** to **P** ratio were synthesized and characterized by various techniques. No significant change of surface area and XRD pattern was observed suggesting that the support was not affected during preparation and no new crystalline phases were formed. The EPR spectra suggest that paramagnetic $V^{+4}$ species are present in all the V-based samples. Furthermore, the amount of $V^{+4}$ species increases with phosphorous content in the modified catalysts. The TPR studies also reveal that $V^{+5}$ and $V^{+4}$ species are present and a new species is formed for the sample containing **V** to **P** ratio of 1:2. The TPR profile also suggests that the reducibility of the surface $V^{+5}$ species is affected since the $T_{max}$ temperature increases with phosphorous content. The $T_{max}$ temperature is similar for the catalysts containing **V** to **P** ratio of 2:1 and 1:1. The EPR spectra were also similar for these two samples. The propane ODH reaction revealed that the conversion and selectivity are inversely related for all catalysts. At constant contact time the conversion decreased with increasing phosphorous content. At iso-conversions, however, the propene selectivity and yield increases with phosphorous content.

The kinetic-parameters were successfully estimated for two power-law models and one mechanistic model by minimizing an appropriate chosen determinant.

Minimization is achieved by the application of a genetic algorithm. It was observed that the power-law model considering carbon-oxides as secondary products described the reaction data better. The kinetic-parameters were also obtained for the corresponding Mars van Krevelan model, which appears to be better suited to explain variations in conversion and propene yields. Using the kinetic-parameters the effect of phosphorous modification was explained. With an increase in phosphorous content the pre-exponential factors progressively decrease, thus, the conversion decreases. The decrease in pre-exponential factors is related to the poisoning of the catalytic active sites. The increase in propene yield at iso-conversion with an increase in temperature and phosphorous modification is due to the decrease in the ratio of rate constants due to propene degradation to propene formation, $(k_2+k_3)/k_1$. The decrease in $(k_2+k_3)/k_1$ ratio with phosphorous addition is primarily due to the dissimilar decrease of pre-exponential factors. Thus, with the proper design of the chemical constituents of the catalysts and the operating conditions the propene yield may be increased.

## *5.2 Recommendations*

Based on the present study the following recommendations are offered.

1. Instead of co-precipitation, sequential addition preparation methods may also be tried.
2. *In-situ* characterization studies can be carried out to provide additional information regarding the surface vanadia species and to provide better mechanistic models since reaction intermediates may be observed.
3. Other mechanistic models, such as Langmuir-Hinselwood and Eley-Rideal models may also be used to understand the reaction mechanism better.
4. Other modifiers may be used to see the effect on the kinetic parameters.

**Reference:**


1. H.H. Kung, Advances in Catalysis, 40 (1995) 1.
2. E.A. Mamedov, V.C. Corberan, Appl. Catal. A 127 (1995) 1.
3. F.D. Hardcastle, I.E.Wachs, J. Mol. Catal. 46 (1988) 173.
4. G. Deo, I. E. Wachs, J. Phy. Chem. 95 (1991) 5889.
5. S. S. Chan, I.E. Wachs, L. L. Murrell, L.Wand, W. Keith, J. Phy. Chem. 88 (1984) 5831.
6. M. A. Banares, M. V. Martinez-huerta, X. Gao, J. L. G. Fierro, I. E. Wachs, Catal. Today 61 (2000) 295.
7. L. J.Burcham, G. Deo, X. Gao, I. E. Wachs, Topics in Catal. 11/12 (2000) 85.
8. G. C. Bond, J. P. Zuria, S. Flamerz, P. J. Gellings, H. Boseh, J. G. V. Ommen, B. J. Kip Appl. Catal. 22 (1986) 361.
9. J.G. Eon , R.Olier, J.C. Volta, J. Catal. 145 (1994) 318.
10. H. Eckert, I. E. Wachs, J.Phy Chem. 93 (1989) 6796.
11. X. Gao, M. A. Banares, I. E. Wachs, J. Catal. 188 (1999) 325.
12. Kamalakanta Routray, M. Tech. Thesis, I.I.T., Kanpur (2003).
13. G.G. Cortez, M.A. Banares, J. Catal. 209 (2002) 197.
14. A. Christodoulakis, M. Machli, A. A. Lemonidou, S. Boghosian, J. Catal. 222 (2004) 293.
15. A. A. Lemonidou, L. Nalbandian, I. A. Vasalos, Catal. Today 61 (2000) 333.
16. F. Arena, F. Frusteri, A. Parmaliana, Catal. Lett. 60 (1999) 59.
17. B. Grzybowska, P. Mekss, R. Grabowski, K. Wcisto, Y. Barbaux, L. Gengembre, Stud. Surf. Sci. Catal. 82 (1994) 151.

18. B. Grzybowskaa, J. Słoczy´nski, R. Grabowski, K. Samsona,I. Gressel, K. Wcisło, L. Gengembre, Y. Barbaux, Appl. Catal. A 230 (2002) 1.

19. Arthur R.J.M. Mattos, Rosane Aguiar da Silva San Gil,Maria Luiza M. Rocco, Jean-Guillaume Eon, J. Mol. Catal. A 178 (2002) 229.

20. G. Deo, I. E. Wachs, J. Catal. 146 (1994) 335.

21. G.Deo, I. E. Wachs, J. Haber, Cri. Rev. Surf. Chem. 4(3/4) (1994) 141.

22. I.E. Wachs, B.M. Weckhuysen, Appl. Catal. A 157 (1997) 67.

23. M. Abon, J.C. Volta, Appl. Catal. A 157 (1997) 173.

24. S.M. Al-Zahrani, N.O. Elbashir, A.E. Abasaeed, M. Abdulwahed, Catal. Lett. 69 (2000) 65.

25. B.Y. Jibril, S.M. Al-Zahrani, A.E. Abasaeed, Catal. Lett. 74 (2001) 145.

26. R.A. Overbeek, P.A. Warringa, M.J.D. Crombag, L.M. Visser,A.J. van Dillen, J.W. Geus, Appl. Catal. A 135 (1996) 209.

27. R.A. Overbeek, A.R.C.J. Pekelharing, A.J. van Dillen, J.W.Geus, Appl. Catal. A 135 (1996) 231.

28. M. Loukah, G. Coudurier, J.C. Vadrine, M. Ziyad, Micro. Mat. 4 (1995) 345.

29. P. Ciambelli, L. Lisi, P. Patrono, G. Ruoppolo, G. Russo, Catal. Lett. 82 (2002) 243.

30. L. Lisi, P. Patrono, G. Ruoppolo, Catal. Lett. 72 (2001) 207.

31. L. Savary, J. Saussey, G. Costentin, M.M. Bettahar, M. Gubelmann-Bonneau, J.C. Lavalley, Catal. Today 32 (1996) 57.

32. P. Ciambelli, P. Galli, L. Lisi, M.A. Massucci, P. Patrono, R. Pirone, G. Ruoppolo, G. Russo, Appl. Catal. A 203 (2000) 133.

33. Reddy, K.R.S.K., M.Tech Thesis, IIT Kanpur (2002).

34. M. Nakamura, K. Kawai, Y. Fujiwara, J. Catal. 34 (1074) 345.

35. R.L. Varma, D.N. Saraf, Ind. Chem. Eng. 20 (1978) 42.

36. M.A. Chaar, D. Patel, H.H. Kung, J. Catal. 109 (1998) 463.

37. D. Creaser, B. Andersson, R.R. Hudging, P.L. Silveston, Canadian J. Chem. Engg. 78 (2000) 182.

38. G. Matra, A. Franco, C. Salvatore, F. Franco, P. Adolfo, Catal. Today 63 (2000) 197.

39. K. Chen, A. Khodakov, Jung Yang, A.T. Bell, E. Iglesia, J. Catal. 181 (1999) 205.

40. R.H.H Smits, PhD Thesis, Universiteit Twente (1994).

41. D. Wolf, S. Moros, Chem. Engg. Sci. 52 (1997) 1189.

42. L. Elliott, S.D. Harris, D.B. Ingham, C.V. Wilson, Compt. Methods Appl. Mech. Engg. 190 (2000) 1065.

43. T. Park, G.F. Froment, Computers. Chem. Engg. 22 (1998) 103.

44. G.E.P. Box, N.R. Draper, Biometrika 52 (1965) 355.

45. I.F. Boag, D.W. Bacon, J. Downie, Cana. J. Chem. Engg. 56 (1978) 389.

46. S. Vajda, P. Valko, Comp. Chem. Engg. 10(1) (1986) 49.

47. R. Mezaki, J.B. Butt, I & EC fundamentals 7(1) (1968) 120.

48. S. M. Shivaji, M.Tech Thesis, IIT Kanpur, (2002).

49. K. Routray, K.R.S.K. Reddy, G. Deo, accepted in Appl. Catal. A.

50. K. Routray, G. Deo, submitted.

51. K. Deb, Optimization for Engineering Design, Prentice-Hall of India Private Limited, 3rd Edition, New Delhi, 1998.

52. D.E. Goldberg, Genetic Algorithm in Search, Optimization and Machine Learning, Addision Wesley, Reading, MA, U.S.A. (1989).

53. J. H. Holland, Adaption in Natural and artificial System, University of Michigan Press, Ann Arbor, U.S.A. (1975).

54. W. A. Dietz, J. Gas Chrom. February (1967).

55. G. F. Froment, K. B. Bischoff, Chemical Reactor Analysis and Design, 2nd Edition, New York, (1990).

56. G. E. P. Box, W. G. Hunter, J. F. MacGregor, J. Erjavec, Technometrics 15(1) (1973) 33.

57. Kangal: http://www.iitk.ac.in/kangal/soft.htm.

58. D. G. Watts, Can. J. Chem. Eng. 72 (1994) 701.

59. D. J. Pritchard, D. W. Bacon, Chem. Eng. Sci. 33 (1978) 1539.

60. G. Kang, D. M. Bates, Biometrika 77 (1990) 321.

61. K. Bahranowski, R. dula, F. Kooli, E.M. Serwicka, Colloids Surfaces A 158 (1999) 129.

62. H. S. Fogler, Elements of Chemical Reaction Engineering, 2nd Edition, Prentice-Hall of India Pvt. Ltd, New Delhi (2003).

# Appendices

# Appendix 1 - Contact Time Studies

**Table A1.1: G.C. areas of propane ODH for 3VTi catalyst**
**Weight of the catalyst = 0.05 g; Temperature = 643 K; Propane: Air =2:1**

| Total Flow Rate (ml/min) | Contact Time (kg $m^{-3}$s) | Raw Areas | | | |
|---|---|---|---|---|---|
| | | $C_3H_8$ | $C_3H_6$ | $CO_2$ | CO |
| **120** | **25** | **1601.374** | **16.395** | **4.011** | **5.137** |
| 120 | 25 | 1212.373 | 13.215 | 3.142 | 4.09 |
| **90** | **33.33** | **1594.509** | **20.018** | **5.355** | **6.763** |
| 90 | 33.33 | 1477.663 | 17.688 | 4.817 | 5.949 |
| **75** | **40** | **1496.8** | **20.605** | **5.832** | **6.839** |
| 75 | 40 | 1405.502 | 18.045 | 5.476 | 6.633 |
| 45 | 66.67 | 1434.023 | 24.003 | 9.167 | 10.934 |
| **45** | **66.67** | **1434.023** | **24.003** | **9.936** | **11.3** |
| 30 | 100 | 1305.38 | 26.454 | 13.392 | 15.509 |
| **30** | **100** | **1380.023** | **28.374** | **14.285** | **16.293** |
| 20 | 150 | 1195.688 | 29.593 | 26.323 | 28.884 |
| **20** | **150** | **1361.981** | **34.265** | **30.539** | **34.782** |

* The values used in the study are marked as bold.

**Table A1.2: G.C. areas of propane ODH for 2V1PTi catalyst**
**Weight of the catalyst = 0.05 g; Temperature = 643 K; Propane: Air =2:1**

| Total Flow Rate (ml/min) | Contact Time (kg $m^{-3}s$) | Raw Areas | | | |
|---|---|---|---|---|---|
| | | $C_3H_8$ | $C_3H_6$ | $CO_2$ | CO |
| **120** | **25** | **1596.891** | **13.399** | **2.254** | **2.656** |
| 120 | 25 | 1471.232 | 12.37 | 1.925 | 2.369 |
| 90 | 33.33 | 1101.959 | 10.728 | 1.861 | 2.054 |
| **90** | **33.33** | **1571.772** | **15.502** | **2.929** | **3.081** |
| **75** | **40** | **1541.986** | **16.432** | **3.172** | **3.447** |
| 75 | 40 | 1327.771 | 14.174 | 2.597 | 2.825 |
| **45** | **66.67** | **1523.409** | **22.329** | **4.593** | **5.338** |
| 45 | 66.67 | 1503.48 | 21.655 | 4.696 | 5.273 |
| 30 | 100 | 1487.146 | 26.952 | 6.887 | 7.707 |
| **30** | **100** | **1471.221** | **26.69** | **6.785** | **7.631** |
| **20** | **150** | **1393.364** | **31.817** | **9.946** | **10.867** |
| 20 | 150 | 1248.722 | 28.002 | 8.699 | 9.328 |

* The values used in the study are marked as bold.

**Table A1.3: G.C. areas of propane ODH for 1V1PTi catalyst**
**Weight of the catalyst = 0.10 g; Temperature = 643 K; Propane: Air =2:1**

| Total Flow Rate (ml/min) | Contact Time (kg $m^{-3}s$) | Raw Areas | | | |
|---|---|---|---|---|---|
| | | $C_3H_8$ | $C_3H_6$ | $CO_2$ | CO |
| 120 | 50 | 1418.311 | 12.325 | 2.176 | 2.141 |
| **120** | **50** | **1565.982** | **13.417** | **1.87** | **2.45** |
| **90** | **66.67** | **1441.876** | **14.458** | **2.195** | **2.66** |
| 90 | 66.67 | 1551.914 | 15.471 | 2.39 | 2.774 |
| **75** | **80** | **1576.641** | **17.551** | **3.021** | **3.446** |
| 75 | 80 | 1525.204 | 16.494 | 2.811 | 3.175 |
| **45** | **133.33** | **1518.463** | **23.631** | **4.805** | **5.313** |
| 45 | 133.33 | 1503.903 | 22.988 | 4.885 | 5.228 |
| **30** | **200** | **1532.229** | **30.737** | **7.497** | **8.245** |
| 30 | 200 | 1473.503 | 29.028 | 7.175 | 7.716 |
| **20** | **300** | **1462.65** | **37.084** | **11.236** | **11.784** |
| 20 | 300 | 1439.391 | 35.981 | 10.582 | 11.467 |

* The values used in the study are marked as bold.

**Table A1.4: G.C. areas of propane ODH for 1V2PTi catalyst**
**Weight of the catalyst = 0.20 g; Temperature = 643 K; Propane: Air =2:1**

| Total Flow Rate (ml/min) | Contact Time (kg $m^{-3}s$) | Raw Areas | | | |
|---|---|---|---|---|---|
| | | $C_3H_8$ | $C_3H_6$ | $CO_2$ | CO |
| 120 | 100 | 1573.121 | 10.568 | 1.251 | 1.2 |
| **120** | **100** | **1595.281** | **9.688** | **1.052** | **1.05** |
| 90 | 133.33 | 1595.128 | 12.194 | 1.398 | 1.447 |
| **90** | **133.33** | **1587.25** | **11.673** | **1.289** | **1.337** |
| 75 | 160 | 1581.675 | 13.579 | 1.585 | 1.523 |
| **75** | **160** | **1564.452** | **12.955** | **1.48** | **1.612** |
| **45** | **266.67** | **1535.337** | **18.294** | **2.221** | **2.33** |
| 45 | 266.67 | 1461.737 | 17.105 | 2.204 | 2.272 |
| 30 | 400 | 1439.74 | 21.781 | 3.748 | 3.447 |
| **30** | **400** | **1498.431** | **23.106** | **3.514** | **3.574** |
| 20 | 600 | 1334 | 26.618 | 5.008 | 4.855 |
| **20** | **600** | **1435.21** | **28.418** | **5.483** | **5.277** |

* The values used in the study are marked as bold.

# Appendix 2 – Reproducibility Studies

**Table A2.1: G.C. areas of propane ODH for 3VTi catalyst**

**Weight of the catalyst = 0.05 g; Total Flow Rate = 75 ml/min;**

**Propane: Air = 1:1**

| Reaction Temperature (K) | Raw Areas | | | |
|---|---|---|---|---|
| | $C_3H_8$ | $C_3H_6$ | $CO_2$ | CO |
| **613** | **1037.261** | **6.667** | **2.334** | **2.976** |
| 613 | 993.876 | 5.588 | 1.816 | 2.33 |
| **633** | **1027.055** | **8.575** | **4.049** | **4.723** |
| 633 | 1045.611 | 8.589 | 3.929 | 4.803 |
| **653** | **1001.56** | **12.098** | **7.797** | **9.591** |
| 653 | 991.351 | 12.206 | 7.142 | 9.373 |
| 673 | 981.748 | 18.494 | 15.555 | 20.048 |
| **673** | **999.603** | **18.935** | **16.323** | **20.438** |
| 653 | 849.545 | 11.319 | 6.936 | 8.402 |
| **653** | **876.724** | **10.984** | **6.591** | **8.085** |
| **633** | **1009.184** | **8.621** | **4.013** | **4.888** |
| **613** | **1018.688** | **6.016** | **1.949** | **2.72** |

* The values used in the study are marked as bold.

**Table A2.2: G.C. areas of propane ODH for 1V1PTi catalyst**

**Weight of the catalyst = 0.10 g; Total Flow Rate = 75 ml/min;**

**Propane: Air = 1:1**

| Reaction Temperature (K) | Raw Areas | | | |
|---|---|---|---|---|
| | $C_3H_8$ | $C_3H_6$ | $CO_2$ | CO |
| 613 | 987.571 | 8.107 | 1.521 | 0.922 |
| **613** | **1021.818** | **8.261** | **0.897** | **1.045** |
| 633 | 1021.946 | 12.911 | 1.854 | 2.432 |
| **633** | **1013.426** | **13.107** | **1.982** | **2.399** |
| **653** | **992.602** | **18.946** | **4.431** | **4.889** |
| 653 | 981.854 | 18.586 | 3.587 | 4.556 |
| **673** | **977.35** | **27.549** | **8.448** | **9.926** |
| 673 | 946.644 | 25.917 | 7.621 | 9.201 |
| **653** | **975.633** | **18.28** | **3.094** | **4.285** |
| 653 | 948.164 | 16.699 | 2.944 | 3.854 |
| **633** | **898.393** | **11.121** | **1.24** | **1.789** |
| 633 | 880.618 | 10.623 | 1.079 | 1.634 |
| 613 | 953.939 | 7.326 | 0.656 | 0.659 |
| **613** | **976.887** | **7.649** | **0.577** | **0.874** |
| **673** | **949.195** | **25.356** | **7.373** | **8.645** |

* The values used in the study are marked as bold.

**Table A3.2: G.C. areas of propane ODH for 2V1PTi catalyst**

**Weight of the catalyst = 0.04 g; Total flow rate = 75ml/min**

| $C_3H_8/O_2$ ratio) | Zero Areas | Reaction Temperature (K) | Raw Areas | | | |
|---|---|---|---|---|---|---|
| | | | $C_3H_8$ | $C_3H_6$ | $CO_2$ | CO |
| 1:1 | **1194** | 613 | 1184.76 | 6.357 | 0.991 | 0.955 |
| | | **613** | **1183.64** | **7.133** | **0.869** | **0.935** |
| | | **633** | **1183** | **11.171** | **1.808** | **1.819** |
| | | 633 | 1178.69 | 10.802 | 1.632 | 1.619 |
| | | 653 | 1192.39 | 19.029 | 3.177 | 3.268 |
| | | **653** | **1182.9** | **16.304** | **2.988** | **3.198** |
| | | **673** | **1181.1** | **26.383** | **6.601** | **7.005** |
| | | 673 | 1127.43 | 23.471 | 6.927 | 7.37 |
| 2:1 | **1980** | 613 | 1980.65 | 15.2 | 1.463 | 1.836 |
| | | **613** | **1962.05** | **9.854** | **0.727** | **0.969** |
| | | **633** | **1958.31** | **17.242** | **1.969** | **2.101** |
| | | 633 | 1976.22 | 16.026 | 2.049 | 1.905 |
| | | **653** | **1953.2** | **25.005** | **4.019** | **4.151** |
| | | 653 | 1892.32 | 23.967 | 3.584 | 4.001 |
| | | **673** | **1914.03** | **38.312** | **9.113** | **9.214** |
| | | 673 | 1912.43 | 37.206 | 8.052 | 8.878 |
| 3:1 | **2550** | 613 | 2549.2 | 15.175 | 1.304 | 1.625 |
| | | **613** | **2543.79** | **11.402** | **1.04** | **1.051** |
| | | **633** | **2466.24** | **18.092** | **1.968** | **2.193** |
| | | 633 | 2440.79 | 17.448 | 1.792 | 1.814 |
| | | **653** | **2448.99** | **27.683** | **3.955** | **4.045** |
| | | 653 | 2545.84 | 27.333 | 3.792 | 3.674 |
| | | **673** | **2368.97** | **44.018** | **9.147** | **9.835** |
| | | 673 | 2408.9 | 43.862 | 9.075 | 9.585 |

* The values used in the study are marked as bold.

**Table A3.3: G.C. areas of propane ODH for 1V1PTi catalyst**

**Weight of the catalyst = 0.10 g; Total flow rate =75ml/min**

| $C_3H_8/O_2$ ratio) | Zero Areas | Reaction Temperature (K) | Raw Areas | | | |
|---|---|---|---|---|---|---|
| | | | $C_3H_8$ | $C_3H_6$ | $CO_2$ | CO |
| 1:1 | 1100 | 613 | 1108.12 | 8.091 | 1.1241 | 1.456 |
| | | **613** | **1136.58** | **7.926** | **0.876** | **1.163** |
| | | **633** | **1134.19** | **11.71** | **2.102** | **2.147** |
| | | 633 | 1144.34 | 12.11 | 2.006 | 2.07 |
| | | 653 | 1062.27 | 16.514 | 4.857 | 4.484 |
| | 1071 | **653** | **1118.24** | **16.474** | **3.625** | **4.098** |
| | | 673 | 1101.81 | 28.328 | 6.898 | 7.504 |
| | | **673** | **1110.3** | **25.709** | **6.513** | **7.333** |
| 2:1 | **1960** | 613 | 1941.15 | 14.368 | 1.87 | 1.852 |
| | | **613** | **1945.04** | **11.649** | **1.093** | **1.221** |
| | | **633** | **1911.68** | **17.963** | **2.227** | **2.378** |
| | | 633 | 1895.18 | 16.952 | 2.08 | 2.267 |
| | | 653 | 1836.08 | 25.514 | 5.994 | 5.662 |
| | | **653** | **1859.55** | **25.506** | **4.39** | **4.596** |
| | | **673** | **1800.9** | **39.484** | **9.842** | **10.447** |
| | | 673 | 1795.26 | 38.825 | 9.624 | 10.001 |
| 3:1. | **2450** | 613 | 2289.9 | 13.019 | 1.347 | 1.199 |
| | | **613** | **2434.75** | **11.114** | **0.9** | **0.909** |
| | | **633** | **2414.98** | **18.733** | **1.865** | **1.891** |
| | | 633 | 2289.34 | 17.794 | 1.802 | 1.874 |
| | | **653** | **2408.56** | **29.441** | **4.014** | **4.262** |
| | | 653 | 2241.96 | 27.879 | 3.805 | 4.12 |
| | | **673** | **2364.64** | **47.437** | **9.95** | **10.646** |
| | | 673 | 2419.6 | 48.036 | 9.079 | 10.132 |

* The values used in the study are marked as bold.

**Table A3.4: G.C. areas of propane ODH for 1V2PTi catalyst**

| $C_3H_8/O_2$ ratio) | Zero Areas | Reaction Temperature (K) | Raw Areas | | | |
|---|---|---|---|---|---|---|
| | | | $C_3H_8$ | $C_3H_6$ | $CO_2$ | CO |
| 1:1 | **1000** | 613 | 1054.25 | 6.513 | 0.369 | 0.539 |
| | | **613** | **986.501** | **5.103** | **0.244** | **0.365** |
| | | 633 | 1042.68 | 8.229 | 0.495 | 0.797 |
| | | **633** | **965.87** | **7.917** | **0.522** | **0.656** |
| | | 653 | 978.347 | 12.018 | 0.809 | 1.12 |
| | | **653** | **945.592** | **10.933** | **0.811** | **1.138** |
| | | **673** | **938.685** | **16.375** | **1.419** | **1.917** |
| | | 673 | 947.769 | 16.069 | 1.336 | 1.908 |
| 2:1 | **1790** | **613** | **1778.77** | **7.641** | **0.386** | **0.515** |
| | | 613 | 1741.29 | 7.223 | 0.338 | 0.352 |
| | | 633 | 1706.17 | 11.331 | 0.665 | 0.698 |
| | | **633** | **1762.85** | **11.608** | **0.58** | **0.786** |
| | | 653 | 1460.09 | 14.875 | 0.742 | 1.138 |
| | | **653** | **1736.22** | **17.775** | **1.24** | **1.312** |
| | | 673 | 1712.65 | 25.948 | 2.146 | 2.489 |
| | | **673** | **1729.91** | **26.015** | **2.355** | **2.488** |
| 3:1 | **2240** | 613 | 1953.4 | 10.482 | 0.51 | 0.606 |
| | | **613** | **2228.37** | **10.44** | **0.478** | **0.624** |
| | | **633** | **2197.75** | **16.191** | **0.764** | **1.068** |
| | | 633 | 2210.82 | 15.714 | 0.76 | 1.085 |
| | | **653** | **2180.53** | **23.464** | **1.423** | **1.729** |
| | 2225 | 653 | 2193.96 | 22.804 | 1.978 | 1.731 |
| | | 673 | 1949.58 | 29.88 | 2.49 | 2.765 |
| | | **673** | **2165.37** | **33.123** | **2.503** | **2.998** |

**Weight of the catalyst = 0.20 g; Total flow rate =75ml/min**

* The values used in the study are marked as bold.

# Appendix 4 – Modeling Data

**Table A4.1: Input and output mole percentages for 3VTi catalyst**
**Weight of the catalyst = 0.03 g; Total flow rate =75ml/min**

| Temperature (K) | Input mole (%) | | Output mole (%) | | | | C-balance ($C_{out}/C_{in}$) |
|---|---|---|---|---|---|---|---|
| | $C_3H_8$ | $O_2$ | $C_3H_8$ | $C_3H_6$ | $CO_2$ | CO | |
| 613 | 17.36 | 17.36 | 17.2152 | 0.10807 | 0.01593 | 0.0197 | 0.998 |
| 633 | 17.36 | 17.36 | 16.9553 | 0.17281 | 0.02917 | 0.03624 | 0.988 |
| 653 | 17.36 | 17.36 | 16.9525 | 0.25469 | 0.05758 | 0.06894 | 0.994 |
| 673 | 17.36 | 17.36 | 15.5137 | 0.33 | 0.09012 | 0.11404 | 0.917 |
| 613 | 29.57 | 14.79 | 29.3227 | 0.16902 | 0.01891 | 0.02543 | 0.998 |
| 633 | 29.57 | 14.79 | 29.0719 | 0.2627 | 0.0456 | 0.04873 | 0.993 |
| 653 | 29.57 | 14.79 | 29.0711 | 0.40269 | 0.08359 | 0.09708 | 0.999 |
| 673 | 29.57 | 14.79 | 28.2634 | 0.58099 | 0.17035 | 0.19257 | 0.979 |
| 613 | 38.65 | 12.88 | 38.4092 | 0.20362 | 0.02389 | 0.02625 | 0.999 |
| 633 | 38.65 | 12.88 | 38.1241 | 0.31816 | 0.04974 | 0.05361 | 0.996 |
| 653 | 38.65 | 12.88 | 36.8127 | 0.46512 | 0.09345 | 0.10207 | 0.966 |
| 673 | 38.65 | 12.88 | 35.9561 | 0.66975 | 0.19388 | 0.21109 | 0.951 |

**Table A4.2: Input and output mole percentages for 2V1PTi catalyst**

**Weight of the catalyst = 0.04 g; Total flow rate = 75ml/min**

| Temperature (K) | Input mole (%) | | Output mole (%) | | | | C-balance ($C_{out}/C_{in}$) |
|---|---|---|---|---|---|---|---|
| | $C_3H_8$ | $O_2$ | $C_3H_8$ | $C_3H_6$ | $CO_2$ | CO | |
| 613 | 17.36 | 17.36 | 17.2337 | 0.10882 | 0.01159 | 0.01247 | 1 |
| 633 | 17.36 | 17.36 | 17.2243 | 0.17042 | 0.02412 | 0.02427 | 1.003 |
| 653 | 17.36 | 17.36 | 17.2228 | 0.24873 | 0.03986 | 0.04266 | 1.008 |
| 673 | 17.36 | 17.36 | 17.1967 | 0.4025 | 0.08806 | 0.09345 | 1.018 |
| 613 | 29.57 | 14.79 | 29.3093 | 0.15424 | 0.00995 | 0.01326 | 0.996 |
| 633 | 29.57 | 14.79 | 29.2534 | 0.26988 | 0.02695 | 0.02875 | 0.999 |
| 653 | 29.57 | 14.79 | 29.1772 | 0.39138 | 0.05501 | 0.05681 | 1.001 |
| 673 | 29.57 | 14.79 | 28.592 | 0.59967 | 0.12472 | 0.12611 | 0.999 |
| 613 | 38.65 | 12.88 | 38.5561 | 0.18108 | 0.01444 | 0.0146 | 1.002 |
| 633 | 38.65 | 12.88 | 37.3808 | 0.28733 | 0.02733 | 0.03045 | 0.975 |
| 653 | 38.65 | 12.88 | 37.1193 | 0.43965 | 0.05492 | 0.05617 | 0.972 |
| 673 | 38.65 | 12.88 | 35.9065 | 0.69907 | 0.12702 | 0.13658 | 0.949 |

**Table A4.3: Input and output mole percentages for 1V1PTi catalyst**

**Weight of the catalyst = 0.10 g; Total flow rate =75ml/min**

| Temperature (K) | Input mole (%) | | Output mole (%) | | | | C-balance ($C_{out}/C_{in}$) |
|---|---|---|---|---|---|---|---|
| | $C_3H_8$ | $O_2$ | $C_3H_8$ | $C_3H_6$ | $CO_2$ | CO | |
| 613 | 17.36 | 17.36 | 17.1528 | 0.12533 | 0.01777 | 0.01608 | 0.996 |
| 633 | 17.36 | 17.36 | 17.1168 | 0.18517 | 0.03328 | 0.02969 | 0.998 |
| 653 | 17.36 | 17.36 | 16.876 | 0.2605 | 0.05012 | 0.05666 | 0.989 |
| 673 | 17.36 | 17.36 | 16.7562 | 0.40654 | 0.09005 | 0.10139 | 0.992 |
| 613 | 29.57 | 14.79 | 29.3518 | 0.18419 | 0.01511 | 0.01688 | 0.999 |
| 633 | 29.57 | 14.79 | 28.8483 | 0.28403 | 0.03079 | 0.03288 | 0.986 |
| 653 | 29.57 | 14.79 | 28.0617 | 0.4033 | 0.0607 | 0.06354 | 0.964 |
| 673 | 29.57 | 14.79 | 27.1765 | 0.62432 | 0.14839 | 0.14444 | 0.943 |
| 613 | 38.65 | 12.88 | 38.4096 | 0.18371 | 0.01301 | 0.01314 | 0.999 |
| 633 | 38.65 | 12.88 | 38.0978 | 0.30965 | 0.02696 | 0.02733 | 0.994 |
| 653 | 38.65 | 12.88 | 37.9966 | 0.48665 | 0.05802 | 0.0616 | 0.997 |
| 673 | 38.65 | 12.88 | 37.3037 | 0.78412 | 0.14381 | 0.15387 | 0.988 |

**Table A4.4: Input and output mole percentages for 1V2PTi catalyst**

**Weight of the catalyst = 0.20 g; Total flow rate =75ml/min**

| Temperature (K) | Input mole (%) | | Output mole (%) | | | | C-balance ($C_{out}/C_{in}$) |
|---|---|---|---|---|---|---|---|
| | $C_3H_8$ | $O_2$ | $C_3H_8$ | $C_3H_6$ | $CO_2$ | CO | |
| 613 | 17.36 | 17.36 | 17.1211 | 0.0928 | 0.00388 | 0.0058 | 0.992 |
| 633 | 17.36 | 17.36 | 16.763 | 0.14397 | 0.0083 | 0.01043 | 0.975 |
| 653 | 17.36 | 17.36 | 16.4111 | 0.19882 | 0.0129 | 0.0181 | 0.958 |
| 673 | 17.36 | 17.36 | 16.2912 | 0.29778 | 0.02256 | 0.03048 | 0.957 |
| 613 | 29.57 | 14.79 | 29.3919 | 0.13229 | 0.00584 | 0.0078 | 0.998 |
| 633 | 29.57 | 14.79 | 29.1288 | 0.20098 | 0.00878 | 0.0119 | 0.992 |
| 653 | 29.57 | 14.79 | 28.6889 | 0.30775 | 0.01877 | 0.01986 | 0.981 |
| 673 | 29.57 | 14.79 | 28.5846 | 0.45041 | 0.03565 | 0.03767 | 0.982 |
| 613 | 38.65 | 12.88 | 38.4497 | 0.18875 | 0.00756 | 0.00986 | 0.999 |
| 633 | 38.65 | 12.88 | 37.9212 | 0.29272 | 0.01208 | 0.01688 | 0.989 |
| 653 | 38.65 | 12.88 | 37.6242 | 0.42422 | 0.0225 | 0.02733 | 0.985 |
| 673 | 38.65 | 12.88 | 37.3625 | 0.59885 | 0.03957 | 0.04739 | 0.983 |

# Appendix 5 – PL-2 Model

**Table A5.1: Kinetic Parameters for the four catalysts following PL-2 Model**

| Parameter | Units | Catalyst | | | |
|---|---|---|---|---|---|
| | | 3VTi | 2V1PTi | 1V1PTi | 1V2PTi |
| $k_{10}$ | $ml\ STP\ min^{-1}\ (g\ cat)^{-1}\ atm^{-(a1+b1)}$ | 9.51 | 6.50 | 2.80 | 0.97 |
| $k_{20}$ | $ml\ STP\ min^{-1}\ (g\ cat)^{-1}\ atm^{-(a2+b2)}$ | 1.04 | 0.44 | 0.17 | 0.04 |
| $k_{30}$ | $ml\ STP\ min^{-1}\ (g\ cat)^{-1}\ atm^{-(a3+b3)}$ | 0.99 | 0.50 | 0.18 | 0.04 |
| $E_1$ | $kJ\ mol^{-1}$ | 90 | 96 | 94 | 77 |
| $E_2$ | | 72 | 91 | 107 | 62 |
| $E_3$ | | 58 | 65 | 88 | 42 |
| $a_1$ | | 1 | 1 | 1 | 1 |
| $b_1$ | | 0.49 | 0.69 | 0.65 | 0 |
| $a_2$ | | 0.82 | 0.70 | 0.51 | 0.62 |
| $b_2$ | | 0 | 0 | 0 | 0 |
| $a_3$ | | 1 | 1 | 0.72 | 1 |
| $b_3$ | | 0 | 0.55 | 0.25 | 0.92 |
| $P_{m(C_3H_6)}$ | $atm$ | 0.0033 | 0.0033 | 0.0035 | 0.0028 |

*Calculated at $P_{m(C_3H_8)} = 0.2958$ atm, $P_{m(O_2)} = 0.148$ atm, $T_m = 643.16$ K

# Appendix 6 – Modeling Data (Contact Time Study)

**Table A6.1: Input and output mole percentages for 3VTi catalyst**

**Weight of the catalyst = 0.05 g; Temperature = 643 K;**

**$C_3H_8$ : $O_2$ = 2:1**

| Total Flow Rate (ml/min) | Contact Time (kg m$^{-3}$s) | Input mole (%) | | Output mole (%) | | | | C-balance ($C_{out}/C_{in}$) |
|---|---|---|---|---|---|---|---|---|
| | | $C_3H_8$ | $O_2$ | $C_3H_8$ | $C_3H_6$ | $CO_2$ | CO | |
| 120 | 25 | 29.57 | 14.79 | 29.1474 | 0.31268 | 0.06689 | 0.08567 | 0.998 |
| 90 | 33.33 | 29.57 | 14.79 | 29.0225 | 0.38178 | 0.0893 | 0.11278 | 0.996 |
| 75 | 40 | 29.57 | 14.79 | 27.244 | 0.39297 | 0.09726 | 0.11405 | 0.937 |
| 45 | 66.67 | 29.57 | 14.79 | 26.1014 | 0.45778 | 0.1657 | 0.18844 | 0.902 |
| 30 | 100 | 29.57 | 14.79 | 25.1185 | 0.54114 | 0.23822 | 0.27171 | 0.873 |
| 20 | 150 | 29.57 | 14.79 | 24.7901 | 0.65349 | 0.50928 | 0.58003 | 0.873 |

**Table A6.2: Input and output mole percentages for 2V1PTi catalyst**

**Weight of the catalyst = 0.05 g; Temperature = 643 K;**

**$C_3H_8$ : $O_2$ = 2:1**

| Total Flow Rate (ml/min) | Contact Time (kg m$^{-3}$s) | Input mole (%) | | Output mole (%) | | | | C-balance ($C_{out}/C_{in}$) |
|---|---|---|---|---|---|---|---|---|
| | | $C_3H_8$ | $O_2$ | $C_3H_8$ | $C_3H_6$ | $CO_2$ | CO | |
| 120 | 25 | 29.57 | 14.79 | 29.0658 | 0.25554 | 0.03759 | 0.04429 | 0.992 |
| 90 | 33.33 | 29.57 | 14.79 | 28.6086 | 0.29565 | 0.04884 | 0.05138 | 0.978 |
| 75 | 40 | 29.57 | 14.79 | 28.0665 | 0.31338 | 0.0529 | 0.05748 | 0.961 |
| 45 | 66.67 | 29.57 | 14.79 | 27.7284 | 0.42585 | 0.07659 | 0.08902 | 0.954 |
| 30 | 100 | 29.57 | 14.79 | 26.7785 | 0.50902 | 0.11315 | 0.12726 | 0.925 |
| 20 | 150 | 29.57 | 14.79 | 25.3613 | 0.6068 | 0.16586 | 0.18122 | 0.882 |

**Table A6.3: Input and output mole percentages for 1V1PTi catalyst**
**Weight of the catalyst = 0.10 g; Temperature = 643 K;**
**$C_3H_8$ : $O_2$ = 2:1**

| Total Flow Rate (ml/min) | Contact Time (kg m$^{-3}$ s) | Input mole (%) | | Output mole (%) | | | | C-balance ($C_{out}/C_{in}$) |
|---|---|---|---|---|---|---|---|---|
| | | $C_3H_8$ | $O_2$ | $C_3H_8$ | $C_3H_6$ | $CO_2$ | CO | |
| 120 | 50 | 29.57 | 14.79 | 28.5016 | 0.25588 | 0.03118 | 0.04086 | 0.973 |
| 90 | 66.67 | 29.57 | 14.79 | 28.2472 | 0.29506 | 0.03986 | 0.04626 | 0.966 |
| 75 | 80 | 29.57 | 14.79 | 27.761 | 0.31457 | 0.04688 | 0.05295 | 0.95 |
| 45 | 133.33 | 29.57 | 14.79 | 27.3733 | 0.43842 | 0.08146 | 0.08718 | 0.942 |
| 30 | 200 | 29.57 | 14.79 | 26.82 | 0.55361 | 0.11965 | 0.12867 | 0.928 |
| 20 | 300 | 29.57 | 14.79 | 26.1991 | 0.68622 | 0.17647 | 0.19123 | 0.913 |

**Table A6.4: Input and output mole percentages for 1V2PTi catalyst**
**Weight of the catalyst = 0.20 g; Temperature = 643 K;**
**$C_3H_8$ : $O_2$ = 2:1**

| Total Flow Rate (ml/min) | Contact Time (kg m$^{-3}$ s) | Input mole (%) | | Output mole (%) | | | | C-balance ($C_{out}/C_{in}$) |
|---|---|---|---|---|---|---|---|---|
| | | $C_3H_8$ | $O_2$ | $C_3H_8$ | $C_3H_6$ | $CO_2$ | CO | |
| 120 | 100 | 29.57 | 14.79 | 29.0365 | 0.18477 | 0.01754 | 0.01751 | 0.988 |
| 90 | 133.33 | 29.57 | 14.79 | 28.8904 | 0.22262 | 0.0215 | 0.0223 | 0.985 |
| 75 | 160 | 29.57 | 14.79 | 28.4754 | 0.24707 | 0.02468 | 0.02688 | 0.972 |
| 45 | 266.67 | 29.57 | 14.79 | 27.9455 | 0.3489 | 0.03704 | 0.03886 | 0.957 |
| 30 | 400 | 29.57 | 14.79 | 27.2737 | 0.44067 | 0.0586 | 0.0596 | 0.938 |
| 20 | 600 | 29.57 | 14.79 | 26.123 | 0.54198 | 0.09144 | 0.088 | 0.904 |